Interaction of high-energy electrons and photons with crystals

V. N. Baĭer, V. M. Katkov, and V. M. Strakhovenko

Institute of Nuclear Physics, Siberian Division, USSR Academy of Sciences, Novosibirsk

The article reviews current ideas regarding electromagnetic phenomena in single crystals. The treatment is based on the theory developed by the authors, which describes radiation of photons by charged particles and production of electron-positron pairs by photons for any energies of the incident particle and arbitrary orientation of the crystal. Attention is given to the significant enhancement of processes in an oriented single crystal in comparison with an amorphous material. The development of particular electron-photon showers is analyzed. The authors make a comparison of theoretical predictions and experimental data which demonstrates their satisfactory agreement. Practical applications of the phenomena considered are presented.

1. INTRODUCTION

The process of radiation of a photon by a charged particle and creation of an electron-positron pair by a photon in a single crystal when the initial particle is moving at a small angle ϑ_0 to the direction of its axes or planes is changed considerably in comparison with an amorphous medium, as a result of the collective interaction of a certain set of systematically located atoms of the crystal lattice with the incident particle.

This group of questions began to be investigated as long ago as the 50s, when it was established that constructive interference of contributions to radiation (pair production) at different centers is possible (coherent radiation and pair production). For certain angles ϑ_0 and energies the probabilities of coherent radiation and pair production (see Refs. 1 and 2 and references cited therein) differ substantially from the probabilities of independent (incoherent) radiation and pair production on individual centers occurring in an amorphous medium (the Bethe-Heitler mechanism).

In the 70s and 80s it was discovered that the specific interaction of charged particles and photons with crystals is far from exhausted by coherent processes. Special interest is presented by the high energy region (tens of GeV and above). The point is that the probabilities of processes in electric fields created by axes and planes of crystals are determined by the magnitude of these fields in the rest system of the radiating (produced) particle. The latter increase in proportion to the energy, and in this way the crystal turns out to be a unique proving ground where quantum electrodynamics in an intense external field can be investigated.

A specific property of electromagnetic processes in crystals is their energy and orientation dependence. For the moderate energy region the angular width in orientation phenomena on departure from an axis or plane is determined by the Lindhard critical angle $\vartheta_c = (2V_0/\varepsilon)^{1/2}$, where ε is the particle energy and V_0 is the scale of the average potential of the axis (plane) relative to which the angle ϑ_0 is determined. On the other hand, it is well known (see for example Ref. 3, Chapter 1) that the characteristics of the radiation process depend substantially on the relation between the characteristic angle of the radiation $\vartheta_\gamma = m/\varepsilon = 1/\gamma$ (m is the electron mass) and the angle of deflection of the particle in its trajectory $\theta^2 \sim \langle (\Delta v)^2 \rangle = \langle \bar{v}^2 \rangle - \langle \bar{v} \rangle^2$, where $\langle ... \rangle$ denotes averaging over time.[1] A corresponding parameter ρ was introduced in Ref. 4 (see also Ref. 5):

$$\rho = 2\gamma^2 \langle (\Delta v)^2 \rangle. \tag{1.1}$$

We recall that for parameter values $\rho \ll 1$ the radiation has a dipole nature and is formed in a time of the order of the period of motion T, while for $\rho \gg 1$ it has a synchrotron-radiation nature (for frequencies contributing to the intensity) and occurs from a small portion of the trajectory in a time of order $T/\rho^{1/2}$.

The motion of the particle and correspondingly the parameter ρ depend on the value of the entry angle ϑ_0 of the particle into the crystal. For entry angles $\vartheta_0 \lesssim \vartheta_c$ the incident electrons are captured into channels or into low super-barrier states, while for $\vartheta_0 \gg \vartheta_c$ the particles move high above the barrier. In the latter case in calculation of the characteristics of the motion it is possible to use the approximation of a straight-line trajectory, by means of which we obtain from (1.1) the estimate

$$\rho(\vartheta_0) = \left(\frac{2V_0}{m\vartheta_0}\right)^2. \tag{1.2}$$

For entry angles $\vartheta_0 \lesssim \vartheta_c$ the value of the transverse (to the axis or plane) velocity of the particle is $v_\perp \lesssim \vartheta_c$ and we have $\rho \lesssim \rho_c$, where

$$\rho_c = \frac{2V_0\varepsilon}{m^2}. \tag{1.3}$$

We shall now define the high-energy region more specifically by the condition $\rho_c \gg 1$. Equation (1.2) shows that there is an additional characteristic angle in the problem, $\vartheta_V = V_0/m$, for which we have $\rho \sim 1$. It follows from the meaning of the parameter ρ and from Eq. (1.2) that in the high energy region the radiation has a synchrotron-radiation nature for $\vartheta_0 \ll V_0/m$ and is dipole for $\vartheta_0 \gg V_0/m$. Since the condition $\rho_c \gg 1$ means that $\vartheta_V \gg \vartheta_c$, for entry angles $\vartheta_0 \gg \vartheta_V$ the theory of coherent bremsstrahlung turns out to be valid (see Ref. 1, Chapters 1–2, Ref. 2, and also Ref. 6, Chapter 8; the criterion of applicability of coherent bremsstrahlung theory is discussed in Ref. 7); this theory is in essence the Born approximation in the crystal potential and for its applicability one requires (in our terms) simultaneous fulfillment of the condition of dipole radiation and the possibility of use of the straight-line trajectory approximation.

Many features of the processes under discussion—radiation by a charged particle and pair production by a photon in a crystal—are similar to radiation and pair production in the field of a plane electromagnetic wave. This is due to the fact that for ultrarelativistic particles and photons moving

near-axes (planes) the crystal field can be reduced to a flux of incident equivalent photons. Since the description of radiation and pair production in the field of a wave is considerably simpler than in a crystal, this analogy turns out to be extremely useful. We shall write the crystal potential in the form

$$U(\mathbf{r}) = \sum_{\mathbf{q}} G(\mathbf{q}) e^{-i\mathbf{q}\mathbf{r}}. \tag{1.4}$$

The explicit form of $G(\mathbf{q})$ depends on the type of lattice and we do not yet need to know it. In the rest system of the crystal there is only an electric field $\mathbf{E}$. In the coordinate system moving with velocity $\mathbf{v}$ along the direction of entry of the charged particle (photon) $\mathbf{n}$ ($\mathbf{v} = n v$) there is a magnetic field $\mathbf{H} = \gamma_v \mathbf{E} \cdot \mathbf{v} (\gamma_v = (1 - v^2)^{-1/2} \gg 1)$ and, as is well known, the resultant field in this system can be represented with relativistic accuracy in the form of plane waves with a wave vector Q_μ, with $Q_0 = \gamma_v v |q_\parallel|$ and $\mathbf{Q}\cdot\mathbf{n} = -\gamma_v |q_\parallel| (q_\parallel = \mathbf{q}\cdot\mathbf{n})$. The flux averaged over time and over the transverse coordinate is the sum of partial contributions $\mathbf{J}_q$. The latter quantity has the form

$$\mathbf{J_q} = -\mathbf{n} \frac{\gamma_v q_\perp^2}{4\pi\alpha |q_\parallel|} |G(\mathbf{q})|^2, \tag{1.5}$$

where $q_\perp = \mathbf{q} - \mathbf{n}(\mathbf{q}\cdot\mathbf{n})$ and $e^2 = \alpha = 1/137$. In the interaction region, the transverse size of which is of the order $\lambda_c = 1/m = \hbar/mc$ and the longitudinal size—the formation length—in the C system of the incident particle and the equivalent photon is $\sim 2\pi/|q_\parallel|\gamma_v$, there are $N_q \simeq |\mathbf{J}_q|\cdot 2\pi\lambda_c^2/|q_\parallel|\gamma_v$ photons. The effective strength of the interaction is characterized by the parameter

$$\alpha N_{\text{ph}} = \alpha \sum_{\mathbf{q}} N_q \simeq \sum_{\mathbf{q}} |G(\mathbf{q})|^2 \frac{q_\perp^2}{m^2 q_\parallel^2}. \tag{1.6}$$

This parameter is purely classical (it does not contain Planck's constant $\hbar$) and always arises in problems with an external electromagnetic field: the same is true of the parameter ρ discussed above and the parameter ξ^2 in the theory of processes in an intense electromagnetic field (see for example Refs. 8–10). For $\alpha N_{\text{ph}} \ll 1$ the external field can be taken into account on the basis of perturbation theory, and for $\alpha N_{\text{ph}} \gg 1$ we have the limit of a constant field. For estimates it is possible to assume that $|G(\mathbf{q})| \sim V_0, q_\parallel \sim q_\perp \vartheta_0$, and then (cf. (1.2))

$$\alpha N_{\text{ph}} \sim \left(\frac{V_0}{m\vartheta_0}\right)^2. \tag{1.7}$$

Therefore, both in radiation and in pair production at entry angles $\vartheta_0 \sim \vartheta_V$ the effective interaction has an intermediate strength and is not described by the well-known limiting expressions. Furthermore the location of the maximum of the probability of coherent pair production is $\vartheta_{\text{max}} \sim \omega^{-1}$ (ω is the photon energy) and shifts with increase of the energy toward smaller angles. When a value $\vartheta_{\text{max}} \sim \vartheta_V$ is reached, the theory of coherent pair production becomes inapplicable in the region of its maximum. In this sense this theory is completely inadequate in the high energy region. In turn, the constant-field approximation, strictly speaking, describes only one, although very important, point on the orientation curve, namely $\vartheta_0 = 0$. These difficulties have been overcome in the development in Refs. 11–16 of a theory of the radiation by particles of high energy and pair production by photons,

which gives a unified description of these processes for any entry angles ϑ_0 of the incident particle and which includes previously known cases as limiting cases for large angles ($\vartheta_0 \gg \vartheta_V$) and small angles ($\vartheta_0 \ll \vartheta_V$). For small entry angles, in the first approximation, the field of the axis (plane) can be considered constant in the formation length of the radiation (pair) $l_f \sim l_0 = m a_s/V_0$, where a_s is the screening radius of the potential (see Refs. 4, 5, and 17). Here from the general theory there follow also corrections $\sim \vartheta_0^2$ to the constant-field limit which take into account the change of the field in the formation length. In this case calculation of the probabilities reduces to selection of an adequate potential and carrying out appropriate averagings (see Refs. 4, 5, 11, 12, and 18 for radiation and Refs. 13–17, 19–23 for pair production). In radiation and at high energies the characteristic angle ϑ_c may appear in the orientation dependence. This occurs not as a result of the fact that for $\vartheta_0 \lesssim \vartheta_c$ the radiation mechanism changes, but as a consequence of rescattering of the flux of charged particles. On the other hand, in pair production by a photon the energy dependence is due entirely to change of the mechanism of the process and the only characteristic angle in it is $\vartheta_V = V_0/m$. It is clear from this why the assumption used in Refs. 24–26, that capture of the particles of the produced pair into the channeling regime has an important role, has not been confirmed.

It is important that in the high energy region the characteristic lengths in which the radiation or pair production processes occur turn out to be one or two orders of magnitude shorter than in the corresponding amorphous material. In view of this, particular electron-photon showers[27] can develop in oriented crystals. These effects appear especially strongly at small angles ϑ_0.

At the present time an extended series of experimental studies has already been carried out with use of beams of photons and electrons at CERN.[28–34] The experimental data obtained are described quite satisfactorily by the theory.[35]

In deriving the basic relations we shall assume the crystal to be thin (i.e., we shall neglect the change of the distribution function in transverse phase space on passage of particles through the crystal). For validity of this approximation it is necessary that (see the discussion in Ref. 36) the crystal thickness be less than the characteristic dechanneling length and the characteristic length of energy loss L_{ch}:

$$L_{\text{ch}}^{-1} = \frac{I(\varepsilon)}{\varepsilon}, \tag{1.8}$$

where $I(\varepsilon)$ is the total intensity of radiation. On the other hand, for the energy region considered ($\rho_c \gg 1$) in a thick crystal for $\vartheta_0 \lesssim \vartheta_V$ a particular electromagnetic shower necessarily develops (see Refs. 19 and 27). For its description it is necessary to solve the corresponding equations of cascade theory, the kernels of which are the expressions given below which describe the emission of a photons and pair production by a photon.

2. RADIATION OF A PHOTON BY A CHARGED PARTICLE AND PAIR PRODUCTION BY A PHOTON IN A CRYSTAL

The most adequate approach to the problem of radiation by relativistic particles and production of a particle pair by a photon of high energy is the formalism using the operator quasiclassical method developed by two of the present authors (see Ref. 3), since it is applicable in all types of

external fields, including non-uniform and variable fields. In the case of large quantum numbers of the motion (in crystals this situation is realized beginning at $\varepsilon \sim 100$ MeV) this method permits us, proceeding from the exact quantum expressions, to go over after a series of transformations to quantities on the classical trajectory of the particle; here the recoil in radiation of a photon (energy conservation) is taken into account exactly, as also in pair production by a photon. The formulas obtained in the framework of this approach (see Refs. 3, 5, 12, and 37) describe the entire set of spin and polarization phenomena. The summation over the variables characterizing the state of the final particles (except their energy) can be carried out in general form. Then, for example, the spectral distribution of the probability of radiation of a photon by an electron (all particles unpolarized) takes the form

$$d\,w_\gamma = \frac{i\alpha\,d\omega}{2\pi}\int \frac{d\,t\,d\tau}{\tau - i0}$$

$$\times\left[\frac{1}{\gamma^2}+\frac{1}{4}\left(\frac{\varepsilon'}{\varepsilon}+\frac{\varepsilon}{\varepsilon'}\right)(\Delta v(t_2) - \Delta v(t_1))^2\right]e^{-iA},$$

$$(2.1)$$

where

$$A = \frac{\omega\varepsilon\tau}{2\varepsilon'}\left[\frac{1}{\gamma^2}+\frac{1}{\tau}\int_{t_1}^{t_2} ds\,(\Delta v(s))^2 - \left(\frac{1}{\tau}\int_{t_1}^{t_2} d\,s\,\Delta v(s)\right)^2\right];$$

$$(2.2)$$

here $v(t)$ is the particle velocity, $v(t) = v_0 + \Delta v(t)$, v_0 is the average velocity, $t_{1,2} = t \mp \tau/2$, $\gamma = \varepsilon/m$, and $\varepsilon' = \varepsilon - \omega$.

As is well known, there is a relation between the completely differential probabilities of radiation of a photon by a charged particle and the production of a pair by a photon. In our case, in view of the fact that all final particles are emitted forward in a small solid angle, this relation is preserved also after integration over part of the variables. In particular, the distribution in the energy of one of the particles of the pair is obtained from (2.1) by means of the substitution rules

$$\omega \to -\omega, \quad \varepsilon \to -\varepsilon, \quad d\omega \to -\left(\frac{\varepsilon}{\omega}\right)^2 d\varepsilon. \qquad (2.3)$$

Equation (2.1) describes the radiation in a given trajectory. For description of radiation in a crystal it is necessary to carry out a summation of the contributions from all possible trajectories. This extremely complicated problem is radically simplified for $\rho_c \gg 1$, since here the mechanism of radiation in the region of entry angles $\vartheta_0 \lesssim \vartheta_c$, where the trajectories are substantially rectilinear, is of the synchrotron radiation type and has a local nature. Then for the summation it is sufficient to know for a given entry angle ϑ_0 the distribution in the transverse coordinate ρ: $dN(\rho,\vartheta_0) = NF(r,\vartheta_0)d^3r/V$, where V is the volume of the crystal and N is the total number of particles. The function $F(r,\vartheta_0)$ for a thin crystal is directly determined by the entry conditions; for example, in the axial case it has the form

$$F_{ax}(\rho,\vartheta_0) = \int \frac{d^2\rho_0}{s(\varepsilon_\perp(\rho_0))}\vartheta(\varepsilon_\perp(\rho_0) - U(\rho)), \qquad (2.4)$$

where $U(\rho)$ is the continuous potential of the axis, normal-

ized so that $U(\rho) = 0$ at the edge of a cell; U_0 is the depth of the potential well;

$$s(\varepsilon_\perp(\rho_0)) = \int d^2\rho\,\vartheta(\varepsilon_\perp(\rho_0) - U(\rho)),$$

$$\varepsilon_\perp(\rho_0) = \frac{\varepsilon\theta_0^2}{2} + U(\rho_0);$$

here $\vartheta(x)$ is the Heaviside function: $\vartheta(x) = 0$ for $x < 0$ and $\vartheta(x) = 1$ for $x > 0$. We note that the distribution (2.4) for $\varepsilon_\perp(\rho_0) > U_0$ (for superbarrier particles) becomes uniform in the axial case, i.e., the factor $F(r,\vartheta_0)$, which takes into account rescattering of the flux, approaches unity.

In the case $\vartheta_0 \gg \vartheta_c$ in order to find $\Delta v(t)$ in (2.1) we can use the straight-line trajectory approximation. In the potential (1.4) we obtain

$$\Delta v(t) = -\frac{1}{\varepsilon}\sum_q G(q)\frac{q_\perp}{q_\parallel}\exp[-i(q_\parallel t + qr)], \qquad (2.5)$$

where $q_\parallel = q\cdot v$, $q_\perp = q - v(q\cdot v)$, and for an initial photon $v = k/\omega$, where k is the photon momentum and for an initial particle $v = v_0$. It is important that for $\rho_c \gg 1$ there are angles ϑ_0 for which $\vartheta_c \ll \vartheta_0 \ll \vartheta_V$, i.e., the straight-line trajectory approximation is applicable even in the region where the effective strength of the interaction becomes large [see Eqs. (1.2) and (1.7)]. The formulas obtained for these values of ϑ_0 remain valid with decrease of the entry angle down to $\vartheta_0 = 0$, since the mechanism of the radiation (pair production) process does not change here. In regard to the region $\vartheta_0 \gtrsim \vartheta_V$, in it for $\rho_c \gg 1$ the straight-line trajectory approximation is clearly applicable. Now, substituting (2.5) into (2.1), taking into account what has been said above regarding summation over all trajectories, we find

$$d\,W_\gamma = \frac{d\,w_\gamma}{d\,t} = -\frac{i\alpha m^2}{2\pi\varepsilon^2}\,d\omega\int \frac{d^3r}{V}\,F(r,\vartheta_0)\int_{-\infty}^{\infty} \frac{d\tau}{\tau - i0}\,B^{(-)}e^{-iA_1}.$$

$$(2.6)$$

where

$$B^{(\pm)} = \left(\sum_q \frac{G(q)q_\perp}{mq_\parallel}e^{-iqr}\sin q_\parallel\tau\right)^2\left(\frac{\varepsilon}{\varepsilon'}+\frac{\varepsilon'}{\varepsilon}\right) \pm 1,$$

$$A_1 = \frac{m^2\omega\tau}{\varepsilon\varepsilon'}$$

$$\times\left[1+\sum_{q,q'}\frac{q_\perp q'_\perp}{m^2 q_\parallel q'_\parallel}G(q)G(q')e^{-i(q+q')r}\Psi(q_\parallel,q'_\parallel,\tau)\right],$$

$$\Psi(q_\parallel,q'_\parallel,\tau) = \frac{\sin[(q_\parallel + q'_\parallel)\tau]}{(q_\parallel + q'_\parallel)\tau} - \frac{\sin(q_\parallel\tau)}{q_\parallel\tau}\frac{\sin(q'_\parallel\tau)}{q'_\parallel\tau}.$$

$$(2.7)$$

We have gone over to the probability per unit time, which can be done if the crystal thickness L is substantially greater than the formation length l_f of the process. Analysis shows (see Ref. 36) that a region of thicknesses for which the crystal can be considered thin and at the same time $L \gg l_f$ exists at any energies.

Equation (2.6) describes the spectral properties of the radiation for $\vartheta_0 \gg \vartheta_c$ for any values of ρ_c, and for $\vartheta_0 \lesssim \vartheta_c$ it describes the properties if the condition $\rho_c \gg 1$ is satisfied. However, for the total intensity of radiation

974   Sov. Phys. Usp. 32 (11), November 1989

Baĭer et al.   974

$$I(\varepsilon) = \int_0^\varepsilon \omega d W_\gamma$$

the region of applicability of the expression which follows from (2.6) is much broader and coincides with the region of applicability of the quasiclassical approximation. This is due to the fact that at energies for which $\rho_c \lesssim 1$ and the synchrotron radiation description is no longer applicable, for angles $\vartheta_0 \lesssim \vartheta_c$ the classical theory of radiation is valid; here the total intensity of radiation also depends only on the local characteristics of the motion. A more general expression describing the production of a pair by a photon in a crystal is obtained from (2.6) by means of the substitutions (2.3), and in addition it is necessary to omit the factor $F(\mathbf{r}, \vartheta_0)$ since redistribution of the photon flux does not occur:

$$d W_e = \frac{d w_e}{d t} = -\frac{i \alpha m^2 d \mathbf{r}}{2\pi \omega^2} \int \frac{d^3 r}{V} \int_{-\infty}^{\infty} \frac{d\tau}{\tau - i0} B^{(+)} e^{-iA_1}. \quad (2.8)$$

In Eqs. (2.6)–(2.8) we have $\varepsilon' = |\omega - \varepsilon|$, i.e., $\varepsilon' = \varepsilon - \omega$ for radiation and $\varepsilon' = \omega - \varepsilon$ for pair production. Equation (2.8) describes[2] the production of pairs for unpolarized electrons and photons at any energies and entry angles. For production of pairs in the field of planes, where there is a distinguished direction in the problem, effects of photon polarization can appear. Pair production in this case has been discussed in Ref. 37.

The quantities $G(\mathbf{q})$ entering into the formulas obtained above have the form

$$G(\mathbf{q}) = \frac{1}{l^3} \varphi(\mathbf{q}) S_{mnk}, \quad (2.9)$$

where l is the lattice constant: $\mathbf{q} = (2\pi/l)(m,n,k)$; m, n, and k, are integers over which the summation occurs in Σ_q; S_{mnk} is the structure factor. For a lattice of the diamond type fcc(d), which exists in particular in crystals of diamond, silicon, and germanium,

$$S_{mnk}^{(d)} = \left\{1 + \exp\left[i\frac{\pi}{2}(m+n+k)\right]\right\}$$

$$\times (\cos \pi k + \cos \pi m)(\cos \pi n + \cos \pi m), \quad (2.10)$$

while for lattices of the bcc type (W, Fe)

$$S_{mnk}^{(b)} = 1 + \cos[\pi(m+n+k)]. \quad (2.11)$$

The quantity $\varphi(\mathbf{q})$ in (2.9) is the Fourier component of the potential of an individual atom, multiplied by the factor $\exp(-u_1^2 q^2/2)$ which arises on averaging over the thermal vibrations of the crystal lattice; here u_1 is the one-dimensional amplitude of the vibrations. For example, in the case of the Moliere approximation used below, for the potential of an individual atom we have

$$\varphi(\mathbf{q}) = 4\pi Z e^2 \exp\left(-\frac{u_1^2 q^2}{2}\right) \sum_{i=1}^{3} \frac{\alpha_i}{q^2 + b_i^2}; \quad (2.12)$$

here α_i and b_i are the parameters of the Moliere potential (see for example Ref. 3) and Z is the charge of the nucleus.

3. NATURE OF PROCESSES FOR SMALL ENTRY ANGLES $\vartheta \ll V_0/m$

The behavior of the probabilities $d W_\gamma$ and $d W_e$ [(2.6) and (2.8)] for various entry angles and energies of the parti-

cles is determined by the dependence on them of the phase A_1 given in (2.7). We shall estimate it for $\vartheta_0 \ll V_0/m$. For definiteness we shall consider the case in which the momentum of the incident particle lies near a crystallographic axis whose direction we shall take as the z axis of the coordinate system. From (2.9)–(2.12) one obtains an estimate $G(\mathbf{q}) \sim V_0$, and therefore the order of magnitude of the double sum in A_1 is $(V_0/m)^2 (q_\perp/q_\parallel)^2 \cdot \Psi(q_\parallel, q_\parallel, \tau)$, where Ψ is a function defined in (2.7). We shall introduce the notation $\mathbf{q}_t$ for the vectors $\mathbf{q}$ lying in the plane (x,y). For them $q_z = 0$, $q_\parallel \sim \vartheta_0 q_\perp$, $q_\perp \sim q$, and for all remaining vectors $q_\parallel \sim q_\perp \sim q$. Then the contribution to the sum of terms with q_z, $q_z \neq 0$, will be $\sim (V_0/m)^2 \Psi \lesssim (V_0/m)^2$, since $|\Psi| \lesssim 1$ for any values of the arguments. Since $(V_0/m)^2 \ll 1$, this contribution can be neglected.[3] Thus, we keep in the sum only terms with $\mathbf{q}_t$, for which its value is $\sim (V_0/m\vartheta_0)^2 \times \Psi(q_\parallel, q_\parallel, \tau)$. The large value of the phase A_1 leads to an exponential suppression of the probabilities W_e and W_γ, and therefore the characteristic values of the variable τ in the integrals (2.6) and (2.8), which have the meaning of the length (time) of formation of the process, are adjusted in such a way that the quantity $\Psi(q_\parallel, q_\parallel, \tau)$ is compensated by the large factor $(V_0/m\vartheta_0)^2$, i.e., the contribution at small entry angles is from $q_\parallel \tau$, $q_\parallel \tau \ll 1$. Expanding the function Ψ accordingly, we find an approximate expression for A_1 for $\vartheta_0 \ll \vartheta_V$:

$$A_1 = \frac{m^2 \omega \tau}{\varepsilon \varepsilon'} \left\{ 1 - \frac{\tau^2}{3} \sum_{\mathbf{q}_t, \mathbf{q}_t'} \frac{G(\mathbf{q}_t) G(\mathbf{q}_t')}{m^2} \mathbf{q}_t \mathbf{q}_t' \exp\left[-i(\mathbf{q}_t + \mathbf{q}_t')\mathbf{\rho}\right] \right.$$
$$\left. \times \left[1 - \frac{\tau^2}{10}\left((\mathbf{q}_t \mathbf{v})^2 + (\mathbf{q}_t' \mathbf{v})^2 + \frac{2}{3}(\mathbf{q}_t \mathbf{v})(\mathbf{q}_t' \mathbf{v})\right)\right] \right\}; \quad (3.1)$$

here $\mathbf{v}$ is the direction of entry of the initial particle [see (2.5)], $\mathbf{\rho} = \mathbf{r}_t$, and the second term in the square brackets is proportional to ϑ_0^2, since $\mathbf{q}_t \cdot \mathbf{v}$ and $\mathbf{q}_t' \cdot \mathbf{v}$ are proportional to ϑ_0. We note that in the problem the averaged potential of the atomic strings of the crystal appears:

$$U(\mathbf{\rho}) = \sum_{\mathbf{q}_t} G(\mathbf{q}_t) e^{-i\mathbf{q}_t \mathbf{\rho}}; \quad (3.2)$$

indeed, using (3.2), we can rewrite (3.1) in the form

$$A_1 = \frac{m^2 \omega \tau}{\varepsilon \varepsilon'} \left\{ 1 + \frac{\tau^2 \mathbf{b}^2}{3} + \frac{\tau^4}{15}\left[(\mathbf{b}(\mathbf{v}\nabla)^2 \mathbf{b}) + \frac{1}{3}((\mathbf{v}\nabla)\mathbf{b})^2\right] \right\}, \quad (3.3)$$

where $\mathbf{b} = \nabla U(\mathbf{\rho})/m$ and $\nabla = \partial/\partial\mathbf{\rho}$. The terms containing $\mathbf{v}\cdot\nabla$ are small (of order ϑ_0^2), and in (2.6) and (2.8) they can be omitted in the pre-exponential factor; then $A_1 \to A_2 = (m^2 \omega \tau/\varepsilon \varepsilon')[1 + (\tau^2 \mathbf{b}^2/3)]$. Carrying out similar expansions of the quantities $B^{(\pm)}$ and then taking integrals over τ, we represent the probabilities $d W_e$ and $d W_\gamma$ for $\vartheta_0 \ll V_0/m$ in the form

$$d W_{e,\gamma} = d W_{e,\gamma}^F + \left(\frac{m\vartheta_0}{V_0}\right)^2 d W_{e,\gamma}^{(1)}, \quad (3.4)$$

where the quantities $d W_{e,\gamma}^F$ and $d W_{e,\gamma}^{(1)}$ do not depend on ϑ_0, while the term $d W_{e,\gamma}^F$ gives the constant-field limit,[4] and the second term in (3.4) gives a correction to it proportional to $\rho^{-1}(\vartheta_0)$ [see (1.2)]. The quantities $d W_{e,\gamma}^F$ are written especially simply:

$$dW_\gamma^F = \frac{\alpha m^2}{\sqrt{3}\pi} \frac{d\omega}{\varepsilon^2} \int \frac{d^2\rho}{s} F_{ax}(\rho, \vartheta_0)$$

$$\times \left[\left(\frac{\varepsilon'}{\varepsilon} + \frac{\varepsilon}{\varepsilon'} \right) K_{2/3}(\lambda) - \int_\lambda^\infty dy K_{1/3}(y) \right],$$

$$dW_e^F = \frac{\alpha m^2}{\sqrt{3}\pi} \frac{d\varepsilon}{\omega^2} \int \frac{d^2\rho}{s}$$

$$\times \left[\left(\frac{\varepsilon'}{\varepsilon} + \frac{\varepsilon}{\varepsilon'} \right) K_{2/3}(\lambda) + \int_\lambda^\infty dy K_{1/3}(y) \right], \quad (3.5)$$

where $F_{ax}(\rho, \vartheta_0)$ is defined in (2.4), $K_\nu(\lambda)$ is the Macdonald function, and $\lambda = 2m^2\omega/3\varepsilon\varepsilon'|\mathbf{b}|$. The correction terms have a similar although more awkward form [see Refs. 12 and 14]. If we take the well known (see for example Ref. 3) probabilities of processes in a constant field at a given distance from the axis ρ and then carry out averaging over the transverse coordinates (with inclusion of the redistribution of the flux in the radiation problem), we obtain immediately the expressions (3.5), which are the limit of the general formulas (2.6) and (2.8) as $\vartheta_0 \to 0$.

We shall rewrite the argument of the functions $K_\nu(\lambda)$ in the form $\lambda = 2u/3\chi(\rho)$ for the radiation problem, where $u = \omega/(\varepsilon - \omega)$, and in the form $\lambda = 2/(3y(1-y)\varkappa(\rho))$ for the pair production problem, with $y = \varepsilon/\omega$, in which the dependence of λ on the parameters $\chi(\rho)$ and $\varkappa(\rho)$ is brought out:

$$\chi(\rho) = \frac{\varepsilon |\nabla U(\varrho)|}{m^3} = \frac{\varepsilon}{m} \frac{E(\varrho)}{E_0}, \quad \varkappa(\rho) = \frac{\omega}{m} \frac{E(\varrho)}{E_0}, \quad (3.6)$$

where $E_0 = m^2/e \approx 1.32 \cdot 10^{16}$ V/cm and $E(\rho)$ is the local value of the electric field of the axis. The parameters χ and $\varkappa$ are invariants: $\chi(\varkappa) = |(eF_{\mu\nu}Q^\nu)^2|^{1/2}/m^3$, where Q^ν is the 4-momentum of the particle (photon) and $F_{\mu\nu}$ is the electromagnetic field tensor, and they play an important role in description of processes in a constant external field. Indeed, from the properties of the K_ν functions ($K_\nu(z) \simeq (\pi/2z)^{1/2}e^{-z}$ for $z \gg 1$) it follows that radiation of frequencies for which $u \gg \chi$ is suppressed exponentially. Therefore, for example, for $\chi \ll 1$ only soft frequencies with $\omega \ll \varepsilon$ are radiated, and in that case it is possible to neglect the change of the particle energy during radiation and to use the classical de-scription of the process. Thus, the value of the parameter χ determines the magnitude of the quantum effects of recoil in radiation. Similarly the parameter $\varkappa$ is related to the magnitude of the transfer of momentum by the field. For example, in the rest system of the produced pair the ratio of the momentum transferred by the field to a charged particle in a length $\lambda_c = 1/m$ to the mass turns out to be $\sim \varkappa$.

For a given strength of the external field the values of the parameters χ and $\varkappa$ and with them all characteristics of the processes are determined by the energy of the particle. In a crystal these parameters will depend also on the distance to the axis, vanishing together with the field strength for $\rho = 0$ as a result of thermal vibrations, reaching a maximum[5] $\chi_1(\varkappa_1)$ for $|\rho| \approx u_1$ (u_1 is the amplitude of vibrations), and then dropping. At a distance from the axis of the order of the screening radius a_s we have a parameter value $\chi(\varkappa) \sim \chi_s = V_0\varepsilon/m^3 a_s$ ($\varkappa_s = V_0\omega/m^3 a_s$). Thus, the picture of the process in a crystal for $\vartheta_0 \ll V_0/m$ for a fixed energy of the initial particles is the same as in a uniform field $E \approx E(u_1)$ but for a substantially nonmonochromatic beam in which all energies up to the initial energy are present.

Below in specific calculations when not specially stipulated the distribution in the transverse coordinate is assumed to be uniform and the axially symmetric approximation of the potential is used over the entire area S associated with an individual axis:

$$U(x) = V_0 \left[\ln \left(1 + \frac{1}{x+\eta} \right) - \ln \left(1 + \frac{1}{x_0+\eta} \right) \right], \quad x = \frac{\rho^2}{a_s^2}; \quad (3.7)$$

here $x_0^{-1} = \pi a_s^2/S$. For estimates we can assume that $V_0 \approx Ze^2/d$, $\eta \approx 2u_1^2/a_s^2$, and d is the average distance between the atoms of the axis. The parameters of the potential (3.7) are given in Table I. They were obtained by means of a fit (details can be found in Ref. 40) on the basis of a model based on the Moliere potential for an individual atom. Sometimes, for example, for the $\langle 111 \rangle$ axis in crystal structures of the type fcc(d) and bcc, the true potential is with high accuracy axially symmetric with respect to the distinguished axis over the entire region S and in any case has this property at distances from the axis $\lesssim a_s$ where the electric field strength has its greatest value. It must, however, be kept in mind that with increase of the energy we begin to have an appreciable contribution from all larger distances from the axis, where

TABLE I. Potential parameters and certain quantities characterizing radiation and pair production.

Crystal	Axis	T	u_1, Å	V_0, eV	η	a_s, Å	x_0	χ_s, $\varepsilon = 100$ GeV	ρ_c, $\varepsilon = 10$ GeV	r_γ^{max}	ω_t
C(d)	111	293	0.040	29	0.025	0.326	5.5	0.13	2.22	168	30
Si	111	293	0.075	54	0.150	0.299	15.1	0.27	4.14	71	150
Si	110	293	0.075	70	1.145	0.324	15.8	0.32	5.36	81	120
Ge	111	293	0.085	91	0.130	0.300	16.3	0.45	5.97	26	100
Ge	110	280	0.083	110	0.115	0.337	15.8	0.48	8.43	30	70
Ge	110	100	0.054	114.5	0.063	0.302	19.8	0.56	8.77	30	50
W	111	293	0.050	417	0.115	0.215	39.7	2.87	31.94	11	22
W	111	77	0.030	348	0.027	0.228	35.3	2.26	26.65	11	13

T is the temperature on the Kelvin scale; u_1 is the amplitude of thermal vibrations; V_0, η, a_s, and x_0 are the parameters of the potential (3.7); χ_s is the parameter characterizing the magnitude of quantum recoil effects; ρ_c is the parameter determining the multipolarity of the radiation; r_γ^{max} is the estimate of the maximum value of the effect for radiation and ω_t is the photon energy at which the probability of a process in the field of axes is equal to the amorphous value.
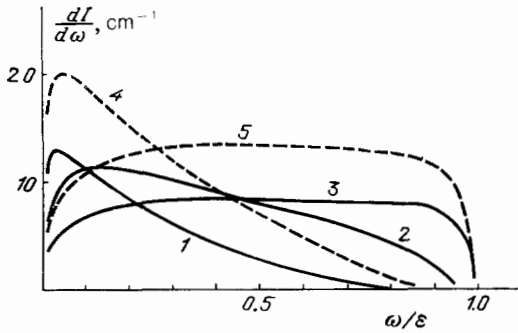
FIG. 1. Spectral intensity of radiation for a given energy in Si ⟨110⟩ ($T = 293$ K; $\varepsilon = 100$ GeV—curve 1, $\varepsilon = 700$ GeV—curve 2, $\varepsilon = 5$ TeV—curve 3) and in Ge ⟨110⟩ ($T = 280$ K; $\varepsilon = 100$ GeV—curve 4 and $\varepsilon = 3$ TeV—curve 5).

FIG. 2. Energy dependence of the total probability of radiation in Si ⟨110⟩ ($T = 293$ K, curve 1), in diamond ⟨111⟩ ($T = 293$ K, curve 2), in Ge ⟨110⟩ ($T = 280$ K, curve 3), and in Ge ⟨110⟩ ($T = 100$ K, curve 4).

the axial symmetry can be destroyed, and then in the averaging in (3.5) it is necessary to use directly the expression (3.2) for $U(\rho)$.

The change of the spectral distribution of intensity $dI^F/d\omega = \omega dW_\gamma^F/d\omega$ with energy can be seen in Fig. 1. It is evident that at an energy $\varepsilon = 100$ GeV the quantity $dI^F/d\omega$ still has a maximum at $\omega/\varepsilon \ll 1$ and drops rapidly with increase of the frequency. However, with increase of the energy the distribution becomes more uniform over the entire spectrum up to $\omega \approx \varepsilon$.

The energy dependence of the total probability of radiation (integrated over frequency) is easily understood by using the estimate $W_\gamma \sim \alpha/l_f$ valid in a constant field; here l_f is the length of formation of the process. Generally speaking, this length will depend on the frequency of the radiated photon (the fraction of the energy carried away by one of the particles in production of a pair by a photon). We shall evaluate it, proceeding from the expression for the phase

$$A_2 = \frac{u}{\chi(\varrho)}\left(1 + \frac{b^2\tau^2}{3}\right)|b|\tau.$$

There is always a contribution from values $|b\tau| \gtrsim 1$, since for $|b\tau| \ll 1$ the quantity $|b|$, which also enters into $\chi(\rho)$, drops out, which corresponds to turning off the field. From the condition $A_2 \sim 1$ we find $l_f \sim \tau \sim 1/|b|$ for $u \sim \chi$ and $l_f \sim (\chi/u)^{1/3}/|b|$ for $u \ll \chi$. The estimate of the total probability involves the value of l_f at frequencies giving the main contribution: $u \sim \chi$ for $\chi \ll 1$ and $u \sim 1$ for $\chi \gtrsim 1$, from which it follows that with increase of the energy the value of W_γ first remains constant and then begins to decrease slowly ($\sim \chi^{-1/3}$). In the case of crystals, where there is an additional averaging over the transverse coordinate, the value of $|b(\rho)|$ at the characteristic distance will enter. In the radiation problem it is the screening radius a_s, and then $l_f \sim l_0(1 + \chi_s^2)^{1/3}$ where $l_0 = ma_s/V_0$. In addition, in the averaging the obvious factor a_s^2/S appears, i.e., in crystals the behavior of the total probability

$$W_\gamma^F = \int_0^\varepsilon d\omega\left(\frac{d W_\gamma^F}{d\omega}\right)$$

can be approximated by the expression

$$W_\gamma^F \approx \frac{\alpha}{l_0}\frac{c_1}{(1+\chi_s^2)^{1/3}}\frac{a_s^2}{S}; \tag{3.8}$$

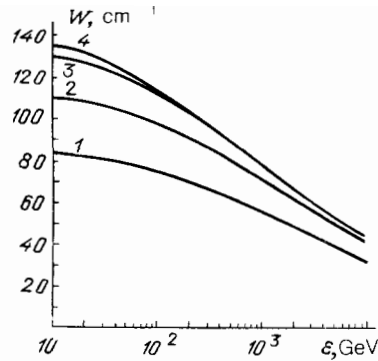here c_1 is a rather large constant; for example, in the poten-

tial (3.7) we have[6] $c_1 \approx 30$. We note further that the value of l_0 is larger for light crystals ($V_0 \sim Z$) and, for example, for the ⟨111⟩ axis varies from $5.7 \cdot 10^{-5}$ cm in diamond to $2.6 \cdot 10^{-6}$ cm in tungsten. At an energy $\varepsilon \sim 10$ TeV the formation lengths in various materials become of the same order: $l_f = 10^{-3}$ cm. The dependence of the probability W_γ^F on energy in various crystals is shown in Fig. 2.

Considerable interest is presented also by the characteristic length in which the particle loses an appreciable fraction of its energy (the analog of the radiation length L_{rad} in an amorphous material), $L_{ch}(\varepsilon) = \varepsilon(I(\varepsilon))^{-1}$; $I(\varepsilon)$ is the intensity of the radiation. In a constant field for $\chi \ll 1$ we have $I(\varepsilon) \sim \varepsilon^2$, and for $\chi \gg 1$ we have $I(\varepsilon) \sim \varepsilon^{2/3}$, and therefore the ratio $I(\varepsilon)/\varepsilon = L_{ch}^{-1}(\varepsilon)$ first rises with energy and then begins to drop, i.e., there is a maximum. In crystals L_{ch}^{-1} behaves in the same way. The dependence of $I^F(\varepsilon)/\varepsilon$ on energy is shown in Fig. 3. Comparison of Figs. 3 and 2 shows that at all energies $W_\gamma^F \gg L_{ch}^{-1}$. This means that the number of photons which carry away an appreciable fraction of the energy and which determine the value of L_{ch}^{-1} is significantly smaller than the total number of photons, which is characterized by the quantity W_γ^F, i.e., a large number of soft photons are radiated. For $\chi_s \gg 1$ an estimate of the type (3.8) is valid for L_{ch}^{-1}, but with a smaller constant, and for the maximum value of this quantity we have
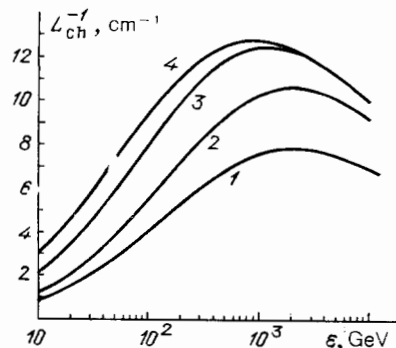

FIG. 3. Energy dependence of the inverse characteristic length of energy loss $L_{ch}^{-1} = I(\varepsilon)/\varepsilon$ in Si ⟨110⟩ ($T = 293$ K, curve 1), in diamond ⟨111⟩ ($T = 293$ K, curve 2), in Ge ⟨110⟩ ($T = 280$ K, curve 3), and in Ge ⟨110⟩ ($T = 100$ K, curve 4).

$$(L_{ch}^{-1})_{max} = c_\gamma \frac{\alpha}{l_0} \frac{a_s^2}{S} .$$ (3.9)

Calculation gives for c_γ values which depend only weakly on the specific material (on the parameter $\eta \sim u_1^2/a_s^2$). For the crystals represented in the table, c_γ varies from 1.3 (Si) to 1.5 (C). We shall give an additional simple estimate of the maximum excess of the radiation length in a corresponding amorphous material over L_{ch}:

$$r_\gamma^{max} = \left(\frac{L_{rad}}{L_{ch}} \right)_{max} \approx \frac{ma_s}{3Z\alpha \ln(183Z^{-1/3})} .$$ (3.10)

Since the values of a_s in different crystals do not differ too strongly, the greatest relative excess is achieved for small Z. The estimate (3.10) is rather rough, and in the table we have given values of r_γ^{max} obtained more accurately.

An important difference of the pair production process from radiation is the presence of a characteristic threshold for small values of x. In a constant field for $x \ll 1$ the production probability is proportional to $\exp(-8/3x)$. In radiation for $\chi \ll 1$ the situation is limited to readjustment of the spectrum (frequencies $\omega \lesssim \varepsilon\chi$ are radiated), whereas in the case of pair production the argument of the functions K_ν in (3.5) is $\lambda = 2/3y(1-y)x(\rho) \geqslant 8/3x$ and for $x \ll 1$ we have $\lambda \gg 1$ for any $y = \varepsilon/\omega$. In this case there is a contribution from the parameter values which provide the minimum value of λ, i.e., in averaging in (3.5) the important region is $|\rho| \sim u_1$, in which the electric field is maximal and the parameter $x(\rho) \approx x_1$, and the spectrum of particles produced is a narrow peak ($\Delta y \sim x_1^{1/2}$) located at $y = 1/2$, so that the two particles carry away identical energy ($\varepsilon = \omega/2$). In accordance with this the total (integrated over ε) probability of pair production by a photon in a crystal for $x_1 \ll 1$ has the form

$$W_e^F = c_2 \frac{\alpha}{l_1} \frac{u_1^2}{S} x_1^{1/2} \exp\left(-\frac{8}{3x_1}\right),$$ (3.11)

which involves the formation length of the process at the corresponding distance from the axis $l_1 = mu_1/V_0$; in the potential (3.7) we have $c_2 \approx 3$. Equation (3.11) describes reasonably well the entire near-threshold region up to $x_1 \sim 1$, when the effect of pair production in the field of the axis becomes appreciable. The estimate of the threshold energy[17] follows from the condition $x_1 \sim 1$

$$\omega_b = \frac{m^3 u_1}{V_0} \sim \frac{m^3 u_1 d}{Z\alpha} ,$$ (3.12)

i.e., the effect appears earliest with increase of the photon energy in materials with large Z and small u_1 and d. Of the crystals used, the minimum value of the threshold energy is reached in tungsten, for which the estimate (3.12) gives $\omega_b \sim 10$ GeV. Since $\omega_b \sim m^3$, production of pairs of heavier particles by a photon as a result of the mechanism discussed can occur only at unachievably large energies; for example, for production of a $\mu^+\mu^-$ pair in tungsten we have $\omega_b(\mu^+\mu^-) \sim 10$ GeV·$(m_\mu/m)^3 \sim 10^8$ GeV. In Table I we have given values of the energy ω_t at which the probability of production of e^+e^- pairs in the field of an axis is compared with the corresponding quantity W_{BH} in an amorphous medium: $W_e^F(\omega_t) = W_{BH}$. The probability $W_e^F(\omega)$ is shown in Fig. 4 for a number of materials in the energy region where
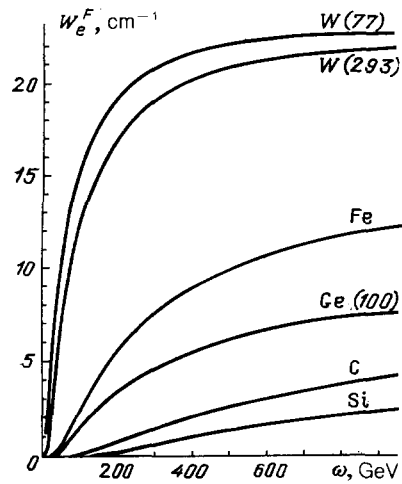

FIG. 4. Probability of production of a pair by a photon for entry angle $\vartheta_0 = 0$ with respect to the $\langle 111 \rangle$ axis (for Ge with respect to the $\langle 110 \rangle$ axis). The numbers in parentheses denote the temperature of the crystal; where they are not given, $T = 293$ K.

its rise is still continuing. On further increase of the photon energy this probability reaches a maximum, after which it drops slowly, so that the general shape of the energy dependence $W_e^F(\omega)$ recalls the plot of $L_{ch}^{-1}(\varepsilon)$ shown in Fig. 3. For the maximum value $(W_e^F)_{max}$ Eq. (3.9) is valid with the difference that $c_\gamma \to c_e$. The constant c_e also depends only weakly on the material, varying from 0.9 to 1.1 for the crystals usually used. The estimate (3.10) for the maximum enhancement of the pair production effect in a field relative to an amorphous medium $r_e^{max} = (W_e^F/W_{BH})_{max}$ also remains valid. The calculated values of r_e^{max} (see Ref. 14) are close to the values of r_γ^{max} given in Table I. With increase of the photon frequency the distribution of the produced particles in energy also changes: the peak at $\varepsilon = \omega/2$ which existed at comparatively low energies gradually goes over into a broad plateau, in the middle of which a dip then appears, which in shape recalls the Bethe-Heitler spectrum. These variations can be traced in Fig. 5.
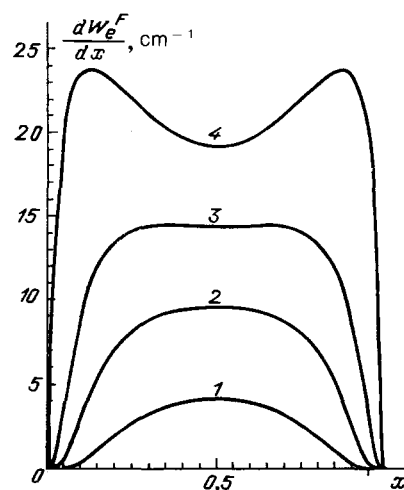

FIG. 5. Distribution in the energy ε of one of the particles of the produced pair ($x = \varepsilon/\omega$) for the $\langle 111 \rangle$ axis in tungsten for $T = 293$ K, $\vartheta_0 = 0$; ω (in GeV) = 25 (curve 1), 50 (curve 2), 100 (curve 3), and 500 (curve 4).
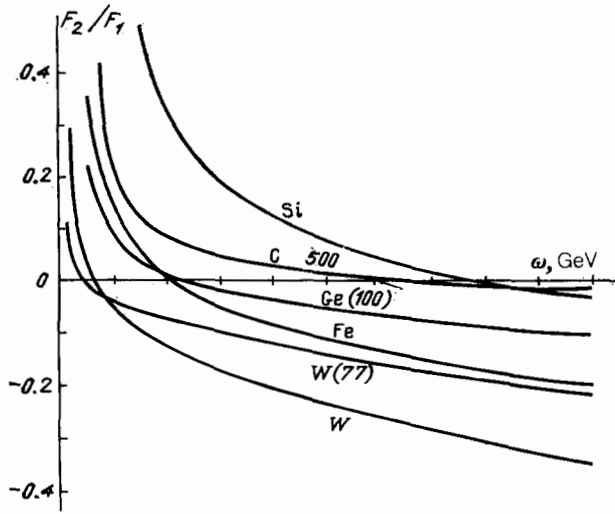
FIG. 6. The ratio $F_2/\widetilde{F}_1$ characterizing the magnitude of the correction to the constant-field limit. The notation is the same as in Fig. 4.

The total probability of pair production for $\vartheta_0 \ll W_0/m$ can be written in accordance with (3.4) in the form $W_e = F_1 + (m\vartheta_0/V_0)^2 F_2$. An idea of the magnitude of the correction can be obtained from Fig. 6, where the ratio F_2/F_1 is given for various materials as a function of energy. Note the fact which is important for understanding the orientation dependence (on the angle ϑ_0): the change of sign of the correction at some energy ω_1, for which[14] it is possible to obtain the following estimate: $\omega_1 \approx \omega_b \cdot (7.2\text{–}7.5)$, where ω_b is the threshold energy defined in (3.12). It is clear that when the quantity F_2 becomes negative with increase of ω, the probability W_e turns out to be (and continues to remain) maximal at $\vartheta_0 = 0$.

4. RADIATION AND PAIR PRODUCTION FOR $\vartheta_0 > V_0/m$

The estimates of the phase A_1 made at the beginning of the previous section remain valid also for $\vartheta_0 \gtrsim \vartheta_V$, except that now the factor in the double sum is $(\vartheta_V/\vartheta_0)^2 \lesssim 1$, so that values $|q_\parallel \tau| \sim 1$ contribute. If $\vartheta_0 \gg \vartheta_V$, then this factor is small, the term with the double sum from A_1 can be moved in Eqs. (2.6) and (2.8) into the pre-exponential part, and then the integrals over τ can be carried out in elementary fashion; here (see Refs. 12 and 14) the formulas of the coherent theory of radiation and pair production in crystals are reproduced.

For $\chi_s(\varkappa_s) \gg 1$ it is possible to obtain from the general formulas (2.6) and (2.8) expressions similar to the formulas of the coherent theory but having a wider range of applicability in the entry angle. Here it is appropriate to use the analogy mentioned above with processes in the field of a plane electromagnetic wave, the probabilities of which depend on the intensity of the wave ξ^2, which characterizes the strength of the interaction (the analog of the parameter ρ; see Eqs. (1.1) and (1.2)), and on the quantity $\lambda = 2Qp/m^2$, where p_μ is the 4-momentum of the particle and Q_μ is the 4-momentum of the wave. According to Ref. 9 for $\lambda \gg 1$ the exact result (without expansion in ξ^2) differs from the Born result ($\xi^2 \to 0$) by the replacement in the principal terms in λ $\lambda \to \widetilde{\lambda} = 2Qp/m_{\text{eff}}^2$, where $m_{\text{eff}}^2 = m^2(1 + \xi^2)$ is the effective mass of the particle in the field of the wave. In a crystal the

value of λ for a given value of q is equal to $2\varepsilon|q_\parallel|/m^2$ and for $|q_\parallel| \sim \vartheta_0/a_s$ we have the estimate $\lambda \sim \chi_s \vartheta_0/\vartheta_V$, i.e., for $\chi_s \gg 1$ this quantity turns out to be large already for $\vartheta_0 \sim \vartheta_V$. From Eqs. (2.6) and (2.8) we find (see Ref. 14 for details of the calculations)

$$\frac{dW_\gamma^{\text{m coh}}}{d\omega} = \frac{\alpha}{4\varepsilon^2}T^{(-)}, \qquad \frac{dW_e^{\text{m coh}}}{d\varepsilon} = \frac{\alpha}{4\omega^2}T^{(+)}, \qquad (4.1)$$

$$T^{(\pm)} = \sum_{\mathbf{q}}|G(\mathbf{q})|^2\frac{q_\perp^2}{q_\parallel^2}\left[\left(\frac{\varepsilon}{\varepsilon'}+\frac{\varepsilon'}{\varepsilon}\right)\pm\frac{4\beta(1-\beta)}{1+(\rho/2)}\right]\vartheta(1-\beta),$$

where

$$\beta = \frac{\omega m_\bullet^2}{2\varepsilon\varepsilon'|q_\parallel|}, \qquad m_\bullet^2 = m^2\left(1+\frac{\rho}{2}\right),$$

$$\frac{\rho}{2} = \sum_{\mathbf{q},q_\parallel\neq0}|G(\mathbf{q})|^2\frac{q_\perp^2}{m^2q_\parallel^2}. \qquad (4.2)$$

The parameter ρ in the form (4.2) is obtained in a calculation in the straight-line trajectory approximation in accordance with the definition (1.1). For tungsten ($T = 293$ K, the $\langle 111 \rangle$ axis) we have from (4.2) $\rho/2 \approx 1.04(V_0/m\vartheta_0)^2$, and for Ge ($T = 100$ K, the $\langle 110 \rangle$ axis) we have $\rho/2 \approx 1.87(V_0/m\vartheta_0)^2$ (compare with the estimate (1.2)). For $\vartheta_0 \gg \vartheta_V$ ($\rho \ll 1$) the expressions of the modified coherent theory (4.1) go over into the formulas of the standard coherent theory.[1,2,6]

Integrating $\omega dW_\gamma^{\text{mcoh}}/d\omega$ (4.1) over frequency, we find for the total intensity of radiation in this approximation

$$I^{\text{m coh}} = \frac{\alpha}{4}\sum_{\mathbf{q}}|G(\mathbf{q})|^2\frac{q_\perp^2}{q_\parallel^2}F(\widetilde{\lambda}), \quad \widetilde{\lambda} = \frac{2\varepsilon|q_\parallel|}{m_\bullet^2}, \qquad (4.3)$$

where

$$F(x) = \left[\ln(1+x)-\frac{x(2+3x)}{2(1+x)^2}\right]\left[1-\frac{8(3+x)}{x^2(2+\rho)}\right]$$
$$+ \frac{x}{(1+x)^2}\left[\frac{8}{2+\rho}+\frac{x(3+2x)}{3(1+x)}\right].$$

The total probability of pair production has the form

$$W_e^{\text{m coh}} = \frac{\alpha}{2\omega}\sum_{\mathbf{q}}|G(\mathbf{q})|^2\frac{q_\perp^2}{q_\parallel^2}f(z)\vartheta(1-z), \qquad (4.4)$$

where

$$z = \frac{2m_\bullet^2}{Qk} = \frac{2m_\bullet^2}{\omega|q_\parallel|},$$

$$f(x) = \left(1+\frac{2x-x^2}{\rho+2}\right)$$

$$\times \ln\frac{1+(1-x)^{1/2}}{1-(1-x)^{1/2}}-\left(1+\frac{2x}{\rho+2}\right)(1-x)^{1/2}.$$

The nature of the spectral distribution is determined by the quantity $\lambda_m = 2\varepsilon|q_\parallel|_{\text{min}}/m_\bullet^2$ (in the case of pair production $\lambda_m = \omega|q_\parallel|_{\text{min}}/2m_\bullet^2$). For definiteness we shall consider the radiation problem, and then for the quantity β from (4.1) with allowance for the convergence of the sum $\Sigma_\mathbf{q}$ we have the estimate $\beta \sim u/\lambda_m$, where $u = \omega/(\varepsilon-\omega)$. If $\lambda_m \lesssim 1$, then frequencies with $u \lesssim 1$ are radiated. With increase of the energy or of the angle ϑ_0 the value of λ_m also rises, and the

spectrum becomes more and more hard. For $\lambda_m \gg 1$ for frequencies $u \sim 1$ we have $(\varepsilon/\varepsilon' + \varepsilon'/\varepsilon) \sim 1$, $\beta \ll 1$ and for $u \sim \lambda_m$ we have $\varepsilon/\varepsilon' + \varepsilon'/\varepsilon \sim u \gg 1$, $\beta \sim 1$, i.e., for $\lambda_m \gg 1$ the spectral distribution has a sharply expressed peak near the kinematic limit at $\omega \approx \varepsilon \lambda_m (1 + \lambda_m)^{-1}$ with a relatively small width $\Delta\omega \sim \varepsilon/\lambda_m$. We emphasize that $\Delta\omega$ does not depend on the energy, since $\lambda_m \sim \varepsilon$. The distribution in the energy of one of the particles in pair production behaves similarly. The only difference is due to the symmetry of this. spectrum relative to the point $y = \varepsilon/\omega = 1/2$ $(\beta^{-1} \sim y(1 - y))$, and therefore for $\lambda_m \gg 1$ there are two peaks: near $y = 1/\lambda_m$ and $1 - y = 1/\lambda_m$ with width $\Delta\varepsilon \sim \omega/\lambda_m$, i.e., one of the particles of the pairs carries away almost the entire energy of the initial photon. Since for all frequencies (energies) for $\lambda_m \gg 1$ the relation $(\varepsilon/\varepsilon') + (\varepsilon'/\varepsilon) \gg \beta$ is satisfied, the expression for $T^{(\pm)}$ in (4.1) is simplified:

$$T^{(\pm)} \underset{\lambda_m \gg 1}{\approx} \left(\frac{\varepsilon}{\varepsilon'} + \frac{\varepsilon'}{\varepsilon}\right) \sum_q |G(q)|^2 \frac{q_\perp^2}{q_\parallel^2} \vartheta(1 - \beta). \qquad (4.5)$$

By means of (4.1) and (4.5) it is easy to estimate the height of the peak. For example, for the intensity spectrum $dI/d\omega = \omega dW_\gamma d\omega$ we find

$$\frac{d I_{max}}{d\omega} \approx \frac{\alpha \rho}{2(2 + \rho)} |q_\parallel|_{min}; \qquad (4.6)$$

this expression, like $\Delta\omega$, does not depend on the energy. We obtain exactly the same estimate for $(dW_e/dy)_{max}$ and $(\varepsilon dW_\gamma/d\omega)_{max}$. The total intensity receives contributions from all frequencies, and not only from the region of the peak, and therefore for $\lambda_m \gg 1$ a weak (logarithmic) dependence on the particle energy is preserved in it. From (4.3) we obtain

$$I^{m \, coh} \underset{\lambda_m \gg 1}{\approx} \frac{\alpha}{8} \rho m^2 \ln \lambda_m. \qquad (4.7)$$

The factor ρm^2 in (4.7) does not depend on the mass of the particle [see (4.2)]. The total probability of radiation for $\lambda_m \gg 1$ differs from (4.7) by the obvious factor ε^{-1}.

The regime of radiation considered can, for sufficiently high energies, be used for creation of a source of hard photons with high monochromaticity. The described behavior of the spectral and total intensity of radiation is typical for undulator radiation in the quantum case in particular and agrees with the results of Ref. 41 (Section 3, Eqs. (34)–(38)). These features of the radiation spectrum are due to the dominant contribution of the lowest harmonics in the equivalent photon spectrum in the case $\lambda_m \gg 1$, and here the discreteness of the spectrum becomes important. This behavior radically distinguishes it from the equivalent photon spectrum in the Bethe-Heitler case, where it is continuous and extends down to arbitrarily low frequencies. As a result both the shape of the spectrum and the energy dependence of the total intensity of radiation differ substantially in these two cases.

A calculation of the radiation in crystals in the framework of coherent bremsstrahlung theory ($\rho \ll 1$) was carried out in Ref. 42 for rather large values $\lambda_m \sim 10$ with allowances for the *spread* in the incident beam. The curves obtained (see Figs. 7 and 8 in Ref. 42) readily demonstrate the features of the radiation spectra discussed above.

We note further that all formulas of the coherent theory

can be easily obtained if one proceeds from the form of the flux $\mathbf{J}_q$ (1.5) and the well known expressions (see for example Ref. 8) for Compton scattering, which is characterized by a cross section $\sigma_{com}(\lambda)$, $\lambda = 2Qp/m^2$, and for two-photon pair production $[\sigma_{\gamma\gamma}(x)$, with $x = 2m^2/Qk]$. For example, the total probabilities found for coherent processes can be represented in the form

$$W_\gamma^{coh} = \sum_q |\mathbf{J}_q| \sigma_{com}(\lambda), \quad W_e^{coh} = \sum_q |\mathbf{J}_q| \sigma_{\gamma\gamma}(x) \vartheta(1 - x)$$

$$(4.8)$$

in complete correspondence with the picture of the phenomenon in terms of equivalent photons. Conversion of the probabilities to the rest system of the crystal corresponds to the replacement $\gamma_v \to 1$ in the expression for the flux $\mathbf{J}_q$ in (1.5). In a similar way we can describe the spectra also, and the existence of $\vartheta(1 - \beta)$ in (4.1) reflects the partial conservation law: $Q + p = k + p'$ for radiation and $Q + k = p + p'$ for pair production.

5. ORIENTATION DEPENDENCE OF THE CHARACTERISTICS OF RADIATION AND PAIR PRODUCTION

The approximate expressions (3.4) and (4.1) given in Sections 3 and 4 for entry angles ϑ_0 which are small and large in comparison with ϑ_V permit determination of the orientation dependence of radiation and pair production processes in a crystal everywhere except in the intermediate region $\vartheta_0 \sim \vartheta_V$. In this region it is necessary, generally speaking, to use the more complicated formulas (2.6) and (2.8), which are valid for any angles ϑ_0. However, in the first approximation, for obtaining the behavior of the curves near $\vartheta_0 \sim \vartheta_V$ we can limit ourselves to the interpolation procedure formulated in Ref. 15.

The nature of the orientation dependence changes with the energy of the initial particle. For example, for the total probability of pair production by a photon, as long as $\omega \ll \omega_b (x_1 \ll 1$; see Eq. (3.12)), the effects of the average field of the axis are small [see Eq. (3.11)] and the specific properties of the crystal appear in the action of the coherent pair production mechanism, which, as follows from (4.4), is nonzero for $\vartheta_0 > \vartheta_V/x_1 \gg \vartheta_V$, when $\rho \ll 1$, and the probability is described by the usual formulas of the coherent theory. In Fig. 7 curve 1 corresponds to the situation in which $x_1 < 1$. With increase of the energy the mechanism of pair production by the averaged field of the axis is turned on, and the maximum in the orientation dependence is shifted toward smaller angles ϑ_0. Curve 2 in Fig. 7 corresponds to the case in which $\omega_b < \omega < \omega_1$, and the maximum is still located at $\vartheta_0 \neq 0$. Finally, for $\omega > \omega_1$ (curve 3 in Fig. 7) the sign of the correction in (3.4) changes, the probability turns out to be greatest at $\vartheta_0 = 0$, and with further rise of the energy the angular width of the peak at $\vartheta_0 = 0$ narrows.

The orientation dependence of the total intensity of radiation at $\vartheta_0 \lesssim \vartheta_c$ in a thin crystal is due to redistribution of the flux of incident particles; in other words, it is due to the change of the distribution function $F(\mathbf{r}, \vartheta_0)$ [see Eq. (2.4)] in the dependence on the angle ϑ_0. This distribution turns out to be different for electrons ($-$) and positrons ($+$), and therefore the radiation for $\vartheta_0 \lesssim \vartheta_c$ will depend on the sign of the charge of the particle. For $\vartheta_0 = 0$ we find from (2.4) for an arbitrary axially symmetric potential (see Ref. 40)
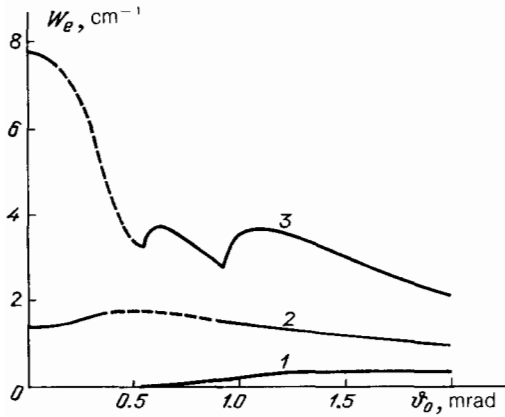
FIG. 7. Orientation dependence of the probability of pair production by a photon in Ge at $T = 100$ K for $\omega = 30$ GeV (curve 1), 100 GeV (curve 2), and 1000 GeV (curve 3). The photon entry angle ϑ_0 is measured with respect to the $\langle 110 \rangle$ axis.

$$F_{ax}^{(-)}(\rho^2, 0) = \ln \frac{x_0}{x}, \quad F_{ax}^{(+)}(\rho^2, 0) = \ln \frac{x_0}{x_0 - x}, \quad x = \frac{\rho^2}{a_s^2}.$$

(5.1)

For $\chi_s \lesssim 1$ there is a contribution to the total intensity from the interval of values $\eta \lesssim x \lesssim 1$, for which $F_{ax}^{(-)} \gtrsim \ln x_0$, $F_{ax}^{(+)} \sim 1/x_0$, from which it follows that in comparison with the case of a uniform distribution in the transverse coordinate the intensity $I^{(-)}$ is enhanced for $\vartheta_0 = 0$ by approximately $\ln x_0$ times, while the intensity $I^{(+)}$ is weakened by approximately x_0 times. With increase of the parameter χ contributions to the intensity come from larger and larger distances from the axis, as a result of which the difference in the intensities for electrons and positrons falls off.

With increase of the angle ϑ_0 from 0 to ϑ_c the distributions $F_{ax}^{(\pm)}(\rho, \vartheta_0)$ gradually approach a uniform distribution, and $F^{(-)}$ changes more rapidly. The total intensity behaves correspondingly (see Refs. 12 and 40), decreasing for electrons from a maximum value $I^{(-)}(0)$ and increasing for positrons from $I^{(-)}(0)$. For $\vartheta_0 \gtrsim \vartheta_c$ the intensities of radiation by electrons and positrons are the same, since $F_{ax}^{\pm}$ $(\rho, \vartheta_0 \gtrsim \vartheta_c) = 1$ [see Eq. (2.4)], and the intensity will depend on the energy. When $\chi_1 \simeq \varepsilon V_0/m^3 u_1 \ll 1$ in the framework of the classical theory (see Ref. 40) for the intensity $I(\vartheta_0)$ with $\vartheta_0 > \vartheta_c$ a plateau is obtained: $I_{cl}(\vartheta_0 \gtrsim \vartheta_c)$ = const. However, even for $\chi \ll 1$ for sufficiently large angles the applicability of the classical description is destroyed. This follows already from the estimate obtained in Ref. 12 of the characteristic radiated frequencies, which is valid up to values $\chi \sim 1$: $\omega/(\varepsilon - \omega) \sim (1 + \rho^{-1}(\vartheta_0))^{1/2}\chi$. It can be seen that for $\vartheta_0 \gg \vartheta_V (\rho(\vartheta_0) \ll 1)$ frequencies with $\omega \sim \varepsilon$ are radiated, and the process cannot be described classically. At the same time for $\rho(\vartheta_0) \ll 1$ the coherent theory is already valid and the intensity is given by Eq. (4.3), if in it we set $\rho = 0$. The formal limit of the expression obtained in this way as $\vartheta_0 \rightarrow 0$ ($z \ll 1$, $F(z) \sim z^2$) gives for the total intensity the classical expression $I_{cl}(\vartheta_0 \gtrsim \vartheta_c)$, and therefore for $\chi_1 \ll 1$ the behavior of $I(\vartheta_0)$ is described by the formulas of coherent bremsstrahlung theory for all angles $\vartheta_0 \gtrsim \vartheta_c$. The next terms of the expansion in z determine the quantum corrections, and as the result of the extra power of $|q_{\parallel}|$ ($z \sim |q_{\parallel}|$) in the numerator the convergence of the sum of the type (4.3) will
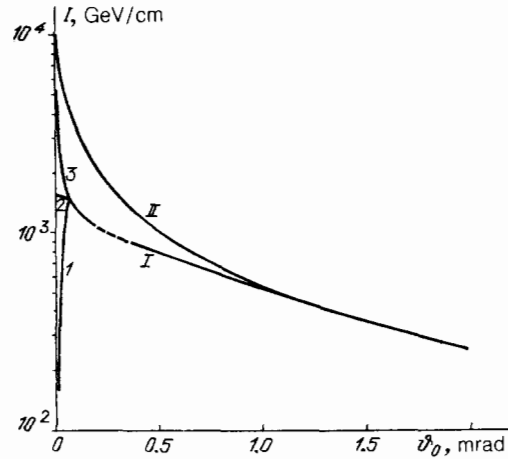

FIG. 8. Orientation dependence of the intensity of radiation in Ge $\langle 110 \rangle$ ($T = 100$ K); $\varepsilon = 150$ GeV. Curve I was obtained in accordance with the formulas of the present work. Curve 1—for positrons, curve 3—for electrons, curve 2—for a uniform distribution. Curve II was obtained with the formulas of standard coherent bremsstrahlung theory.

be assured [see Eqs. (2.9) and (2.12)] by the factor $\exp(-q^2 u_1^2)$, i.e., values $|q_{\parallel}| \sim \vartheta_0/u_1$ will contribute. The relative magnitude of the correction terms is given by the characteristic value $z \sim \varepsilon |q_{\parallel}|/m^2 \sim \varepsilon \vartheta_0/u_1 m^2 \approx \chi_1 \vartheta_0/\vartheta_V$. It becomes large at $\vartheta_0 \sim \vartheta_V/\chi_1$, which also determines the angular size of the plateau in the behavior of $I(\vartheta_0)$. With increase of the energy this plateau narrows and for $\chi_1 \sim 1$ it disappears completely.

The typical form of the orientation dependence of the intensity of radiation by electrons and positrons at $\chi_s \sim 1$ in a thin crystal is given in Fig. 8. Curve I was obtained with the formulas given above. It can be seen that for $\vartheta_0 < \vartheta_c$ the intensity depends substantially on the type of particle and on the angular width of the beam $\Delta\vartheta_0$: curves 1 and 3 respectively describe the intensities of radiation by positrons and electrons (with $\Delta\vartheta_0 = 0$). Curve 2 describes the case of a uniform distribution over the coordinates, which corresponds to a large angular spread in the incident beam ($\Delta\vartheta_0 \sim \vartheta_c$). For $\vartheta_0 > \vartheta_c$ the three curves merge into a single curve. Curve II in Fig. 8 was plotted from the standard theory of coherent bremsstrahlung. From comparison of it with curve I it is possible to make deductions regarding the region of applicability of this theory for $\chi \sim 1$. Already at these values of χ the quantum effects of recoil have become dominant. In Fig. 8 this was expressed in the large difference of the intensity values for $\vartheta_0 = 0$ between curve II (agreement at this point with the classical value) and curve 2.

6. ELECTRON-PHOTON SHOWERS IN ORIENTED CRYSTALS

If the thickness of the crystal turns out to be comparable with the characteristic length of energy loss $L_{ch}(\varepsilon)$ determined in (1.8), or when the initial particle is a photon with length $W_e^{-1}(\omega)$ in which pair production occurs with an appreciable probability, then an electromagnetic cascade is developed in a crystal. At the same time in this case already one cannot, as was done for thin crystals, neglect the change of the distribution function with penetration of the particle beam deep into the crystal. The main processes determining the change of the distribution function are multiple scatter-

ing and radiation loss. The relative role of these processes in the kinetics will in turn depend on the energy. Indeed, the quantity $L_{ch}(\varepsilon)$ drops with energy up to $\varepsilon \sim 1$ TeV, where (see Fig. 3) it reaches a minimum value, while the dechanneling length $l_d(\varepsilon)$

$$l_d(\varepsilon) = \frac{\alpha}{2\pi} \frac{U_b \varepsilon}{m^2} L_{rad} \qquad (6.1)$$

—the distance in which the rms multiple scattering angle in the corresponding amorphous medium-becomes equal to the Lindhard angle ϑ_c and rises in proportion to ε. Therefore at some energy[36] $\varepsilon = \varepsilon_{cr}$ these lengths become equal: $l_d(\varepsilon_{cr}) = L_{ch}(\varepsilon_{cr})$. For Ge, for example, $\varepsilon_{cr} \approx 40$–60 GeV, depending on the axis and on the temperature. For $\varepsilon < \varepsilon_{cr}$ the effects of multiple scattering dominate in the kinetics, and for $\varepsilon > \varepsilon_{cr}$ radiation loss effects dominate. The analysis carried out in Ref. 6 of the kinetics due to multiple scattering ($\varepsilon < \varepsilon_{cr}$) showed that at large thicknesses $l \gg l_d$ the distribution in the transverse phase space turns out to be uniform. This result has made it possible (see Ref. 36) to solve for $\varepsilon < \varepsilon_{cr}$ the problem of radiation loss in a thick crystal. For $\varepsilon > \varepsilon_{cr}$ the kinetics becomes more complicated, but here also it is frequently justified to use the assumption of a uniform distribution of the particles in the coordinate transverse to the axis. For example, if the angular spread in the incident beam $\Delta\vartheta_0 \sim \vartheta_c$, then already on entry into the crystal most electrons turn out to be in superbarrier states, where $F(\rho, \vartheta_0) = 1$ [see Eq. (2.4)]. Sometimes, in crystals of intermediate thickness, there may also appear substantially the radiation of a small group of electrons captured in the channel. We shall return to this question below, but for now we shall assume the distribution in the transverse coordinate to be uniform for all particles.

The dependence of pair production and radiation in crystals on the entry angle ϑ_0 leads to an orientation dependence and to the development of showers. For the energies considered the opening angle of the particles in the elementary process $\sim 1/\gamma \ll \vartheta_V$, and multiple scattering is suppressed. Therefore we can assume that development of a shower will not occur in the direction of the momentum of the initial particle[7] and is determined by the mechanism associated with a given entry angle ϑ_0. We shall consider showers in the fields of axes[8] ($\vartheta_0 \ll \vartheta_V$), when the enhancement effects are greatest.

The theory of cascade showers in an amorphous material was formulated and developed in Refs. 44–46. These studies obtained kinetic equations which describe the development of the cascade and found an analytic solution in the case in which only radiation and pair production are taken into account,[46] i.e., the Bethe-Heitler characteristics of the processes were used as the kernels in the equations. In recent years a large number of papers have been published on the development of this theory; a review may be found, for example, in Ref. 47.

We note the following features of development of a shower in the field of axes, which distinguish it from the amorphous case and which are due to a change in the crystal of the radiation and pair production processes.

1) The characteristic lengths in which development of a shower occurs can be significantly smaller here than in the corresponding amorphous material (disoriented crystal).

2) There is a rather sharp limit ω_b (3.12) in photon frequency, below which the probability of photoproduction of a pair in the field of an axis drops exponentially. At the same time if the energy of the particle is $\varepsilon \sim \omega_b$, it radiates intensely as a result of the mechanism discussed. 3) Both the pair production probability $W_e^F(\omega)$ and the characteristic energy loss length $L_{ch}(\varepsilon)$ depend on the energy, while for the Bethe-Heitler process the corresponding quantities W_{BH} and L_{rad} are constants. 4) For $\varepsilon \lesssim \omega_b$, as was mentioned above, a large number of relatively soft photons are emitted, which do not affect the energy loss of the particle which radiates them. Nevertheless these photons can produce pairs as a result of the Bethe-Heitler mechanism (i.e., with a relatively low probability). As the result a special shower is developed, which is due to a mixed mechanism, and in which a large number of photons can produce an appreciable number of pairs in spite of the low probability of the photoproduction process. Here, naturally, the number of photons in the shower will substantially exceed the number of charged particles. It is necessary to distinguish hard showers, in which the energy is $\varepsilon \gg \omega_b$, and soft showers, in which $\varepsilon \lesssim \omega_b$

An analysis of electron-photon showers in the fields of crystal axes in the case of a uniform distribution was carried out in Ref. 27. For a hard shower it was possible to obtain an analytic solution of the kinetic equations. As is well known, the number of particles in a shower with energy above a certain value rises exponentially up to an optimal thickness $t = t_{op}$. We shall give here only the explicit expressions for solutions near t_{op}, which is given by the expression

$$t_{op} = \frac{2}{5} \int_0^\eta dy \left(\frac{1}{a(y)} + \frac{1}{b(y)} \right), \qquad (6.2)$$

where we have introduced the following variables and functions:

$$\eta = \ln \frac{\omega_n}{\omega}, \quad \zeta = \ln \frac{\omega_0}{\varepsilon}, \quad a(\zeta) = L_{ch}^{-1}(\omega_0 e^{-\zeta}),$$

$$b(\eta) = W(\omega_0 e^{-\eta}), \quad N(\omega, t) = \frac{1}{\omega_0} N(\eta, t); \qquad (6.3)$$

here ω_0 is the energy of the initial particle, for example, a photon. Near $t = t_{opt}$ the number of photons (electrons) with energy η, $N_\gamma(\eta, t)$ or $N_e(\eta, t)$, has the form of a Gaussian distribution in time (depth):

$$N_\gamma(\eta, t) = \frac{2e^m}{5(2\pi d)^{1/2} b(\eta)} \exp\left[-\frac{(t - t_{op})^2}{2d(\eta)}\right],$$

$$N_e(\eta, t) = \frac{b(\eta)}{a(\eta)} N_\gamma(\eta, t), \qquad (6.4)$$

$$d(\eta) = \frac{4}{125} \int_0^\eta dy \left(\frac{7}{a^2(y)} - \frac{1}{a(y)b(y)} + \frac{17}{b^2(y)} \right).$$

For solution of the problem we made a number of simplifying assumptions which permitted us to take into account in the adiabatic approximation the dependence of the probabilities on the energy. This leads to an error $\lesssim 15\%$, which was monitored by numerical modeling carried out of the hard cascade. If the lower limit of the energy of the detected particles of the cascade is $\varepsilon_f(\omega_f) \ll \omega_b$, then for a sufficient thickness of the crystal at some depth the average energy of the

982   Sov. Phys. Usp. 32 (11), November 1989

Baĭer *et al.*   982

particles turns out to be $\varepsilon(\omega) \lesssim \omega_b$. Then for the most part the Bethe-Heitler mechanism of pair production operates, but the radiation of the particles in the field of a single crystal still remains quite intense ($b \sim W_{BH}, a \gg L_{rad}^{-1}$).

It is clear that the principal number of photons is radiated in a characteristic length

$$l \sim \int\limits_0^\eta \frac{d\,y}{a\,(y)} = \int\limits_0^{\ln\eta} d\,y L_{ch}\,(\varepsilon_0 e^{-y}) \ll t_{op}.$$

Then there is a rather broad interval of t in which the number of photons remains practically constant (dropping off smoothly as the result of absorption) up to a length $t \sim W_{BH}^{-1}$, at which their conversion into pairs becomes appreciable. In the situation considered it is necessary to distinguish two substantially different cases. In the first case the initial energy $\omega_0(\varepsilon_0) \gg \omega_b$ and a mixed cascade develops. In the second case $\omega_0(\varepsilon_0) \sim \omega_b$ and a soft cascade develops.

The mixed cascade was studied by means of numerical modeling. The dependence obtained by this method for the number of charged 1 particles and photons on the shower development depth in a silicon crystal for various energies of the initial photon is given in Fig. 9. The lower limit of photon energy in the cascade was chosen as $\omega_f = 100$ MeV, which corresponds approximately to the effective threshold for photoproduction of an electron-positron pair in matter. It can be seen in Fig. 9 that in accordance with the above statement the number of photons reaches a plateau. The lower limit of the energy of the charged particles was taken as $\varepsilon_f = 10$ GeV. On the one hand, this choice assures applicability of the synchrotron radiation approximation used for description of the radiation. On the other hand, for an energy $\varepsilon < 10$ GeV mainly photons with energy $\omega < \omega_f = 100$ MeV are radiated. In Fig. 10 we have given the dependence of the number of photons N_γ with energy $\omega > 100$ MeV and of the total number of charged particles N_e on the energy of the initial photon ω_0 entering a silicon crystal of thickness $L = 1$ cm at a small angle $\vartheta_0 \ll V_0/m$ to the $\langle 110 \rangle$ axis. It is interesting that the ratio of the number of photons N_γ to the number of charged particles N_e is practically independent of the initial energy and amounts to $N_\gamma/N_e \approx 11$. Dependences similar to those shown in Fig. 10 when used in detection of ultra-

FIG. 10. Total number of charged particles N_e and photons with energy $\omega > 100$ MeV N_γ at a depth of 1 cm in a silicon single crystal ($\langle 110 \rangle$ axis, $T = 293$ K) as a function of the initial photon energy.

high energy photons[48] permit determination of their energy with high accuracy.

The development of a soft cascade reduces mainly to successive radiation of photons by charged particles. In the energy region corresponding to a soft cascade, the total radiation probability $W_\gamma(\varepsilon)$ and the value of $L_{ch}(\varepsilon)$ change very weakly. These properties of the synchrotron radiation mechanism can be used for approximate calculation of certain characteristics of the cascade, which turns out to be extremely useful in view of the complicated nature of a complete calculation of the shower development. One of these characteristics is the average energy of the charged particles in the shower at a given depth $\langle \varepsilon(l) \rangle$. The corresponding approach has been developed in Ref. 18, where it was shown also that taking into account the dispersion of the distribution in ε only slightly changes the result for $\langle \varepsilon(l) \rangle$. In addition, in Ref. 18 the radiation spectrum was found neglecting dispersion, but including the average energy loss. This approximate description of the spectral and total losses turns out to be quite satisfactory. This were confirmed in Ref. 27 by numerical modeling of a soft cascade for the conditions of the experiment of Refs. 29 and 30, in which radiation and pair production were studied in crystals of Ge ($T = 100$ K, the $\langle 110 \rangle$ axis, $\varepsilon_0 = 150$ GeV, $\omega_0 \leq 155$ GeV) of thickness $L = 0.04$ and 0.14 cm. In particular, the values $\langle \varepsilon(0.04) \rangle = 0.66\varepsilon_0$ and $\langle \varepsilon(0.14) \rangle = 0.26\varepsilon_0$ practically coincide with the results of Ref. 18 and the experiment of Refs. 29 and 30. The simple estimates of the number of secondary particles for $1 \lesssim L_{ch} \ll L_{rad}$ also turn out to be useful. For example, for an initial electron in the framework of the approach adopted we have (see Ref. 27) a number of photons at depth l

$$N_\gamma(l) = \int\limits_0^l W_\gamma(t)\,d\,t = \int\limits_{\langle\varepsilon(l)\rangle}^{\varepsilon_0} W_\gamma(\varepsilon) L_{ch}(\varepsilon) \frac{d\,\varepsilon}{\varepsilon}$$

$$= \int\limits_0^\eta \frac{W_\gamma(\varepsilon_0 e^{-y})}{a\,(y)}\,d\,y \equiv \overline{W}_\gamma l, \qquad (6.5)$$

$$\eta = \ln\frac{\varepsilon_0}{\langle\varepsilon(l)\rangle},$$

and for the number of secondary charged particles we obtain

$$N_e(l) = 2 \int\limits_0^l W_e^{BH} N_\gamma(t)\,d\,t = 2W_e^{BH} \int\limits_0^l W_\gamma(t)(l-t)\,d\,t$$

$$\approx W_e^{BH} \overline{W}_\gamma l^2 \approx W_e^{BH} N_\gamma(l)\,l. \qquad (6.6)$$

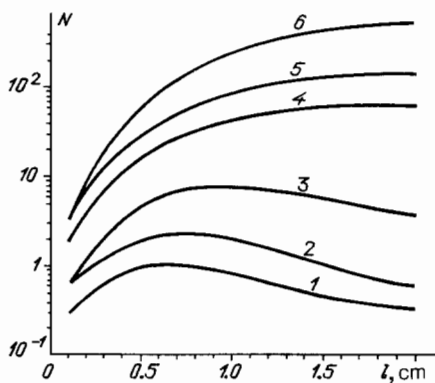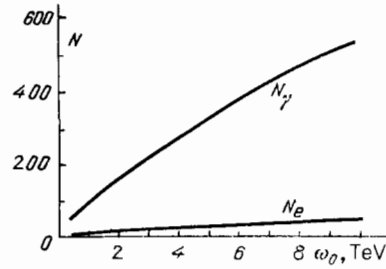For example, under the conditions of the experiment of Refs.

FIG. 9. Number of charged particles with energy $\varepsilon > 10$ GeV in a silicon single crystal ($\langle 100 \rangle$ axis, $T = 293$ K) in the case in which the photon hitting the crystal has energy ω_0 (TeV) = 0.4 (curve 1), 1 (curve 2) and 4 (curve 3). The number of photons with energy $\omega > 100$ MeV for the same conditions is given by curves 4–6 respectively.

29 and 30 the estimates (6.5) and (6.6) give[9] $N_\gamma (0.14) \approx 16.8$, $N_c (0.14) \approx 0.67$ and $N_\gamma (0.04) \approx 4.4$, N_c $(0.04) \approx 0.05$, i.e., many photons are radiated, and for $L = 0.14$ cm the number of secondary charged particles also turns out to be appreciable. Thus, already for these energies the process has a cascade nature. When, as in Ref. 24, the initial particle is a photon, inclusion of the cascade leads to a marked change in the distribution in energy (see Fig. 6 in Ref. 27) of the produced particles as the result of radiation by them of photons, in comparison with what would be observed in a thin crystal.

Let us turn now to the situation in which the distribution in the transverse coordinate cannot be considered identical for all beam particles, which substantially affects the shape of the energy loss spectrum. This was brought out in the experiment of Ref. 31, in which the radiation was investigated in a crystal of Ge($\langle 110 \rangle$ axis, $T = 100$ K, $\varepsilon_0 = 150$ GeV) of thickness $L = 1.85 \cdot 10^{-2}$ cm. For these conditions the dechanneling length is $l_d(\varepsilon_0) = 0.51$ cm, and L_{ch} $(\varepsilon_0) = 0.1$ cm. It must be kept in mind, however, that these values of l_d and L_{ch} were obtained, strictly speaking, for super-barrier motion where $\varepsilon_\perp > U_0$, i.e., any distances from the axes are accessible, and the distribution in the transverse coordinates is uniform. Let us consider particles in a channel with $\varepsilon_\perp < U_0$, in which case their motion occurs in the region $x \leqslant x_1$ [we shall use the potential of (3.7), with $x_0 = 19.8$ and $\eta = 0.063$], where x_1 is given by the equality $U(x_1) = \varepsilon_\perp$. Assuming the distribution in x to be uniform over the entire accessible region of motion, we see that with decrease of $\varepsilon_\perp$ (x_1) the multiple scattering increases in proportion to $(x_0 + \eta)/(x_1 + \eta)$ as the result of increase of the average density of electrons and for $x_1 \sim 1$ can exceed by tens of times $(x_0 \gg 1, \eta \ll 1)$ the similar value for superbarrier electrons. The intensity of radiation increases, although not so rapidly; for example, for $x_1 = 1$ it increases by 12.5 times in comparison with the superbarrier value. Thus, a crystal can be thin for super-barrier electrons and thick for part of the channeled particles. For positrons, with decrease of $\varepsilon_\perp$ from the value U_0, there is a decrease both in the multiple scattering by nuclei and in the intensity of the radiation, since the region of coordinates near the axes becomes less and less accessible for them. Thus, it is necessary to consider a complicated kinetic problem which has not been solved up to this time even without taking radiation into account. Here we shall carry out a qualitative analysis of the situation, tracing the variation of the average value $z = \langle \varepsilon_\perp \rangle / U_0$, assuming that at the initial moment the particles were concentrated at $z = z(0) < 1$. The variation of z and ε is described by the system of equations

$$\frac{dz}{dl} = \frac{1}{l_d(\varepsilon)} \frac{x_0 + \eta}{x_1 + \eta} - f_1(\varepsilon, z), \quad \frac{1}{\varepsilon} \frac{d\varepsilon}{dl} = -f_2(\varepsilon, z), \quad (6.7)$$

where

$$f_1(\varepsilon, z) = \int_0^{x_1} \frac{dx}{x_1} \left(z - \frac{U(x)}{U_0} \right) \frac{I(x)}{\varepsilon}, \quad f_2(\varepsilon, z) = \int_0^{x_1} \frac{dx}{x_1} \frac{I(x)}{\varepsilon}. \quad (6.8)$$

We recall that $I(x)$ is the local value of the total radiation intensity in the field of an axis, and it is convenient to go over in (6.7) to the variable x_1 in accordance with the equality $z = U(x_1)/U_0$. The system of equations (6.7) was solved

(see Ref. 35) with a number of simplifying assumptions. For $\varepsilon_0 = \varepsilon(0) = 150$ GeV the first term in (6.7), which takes into account the effect of multiple scattering, exceeds f_1 for $x_1(0) < 1.3$ ($z(0) < 0.81$), and therefore for particles which have a smaller value of $x_1(0)$, an increase of the average transverse energy begins at once (at $l = 0$). For larger values of $x_1(0)$ the value of $x_1(z)$ first decreases as the result of radiation, but then, as a consequence of decrease of x_1 and, mainly, as the result of the loss of total energy ε, at some depth l an increase of $x_1(z)$ begins. As a result of solution of the system of equations (6.7) it turned out that for particles which lose an appreciable fraction of their total energy, in a relatively thin crystal the "trajectories" $x_1(l)$ traversed a region of values of x which is limited for all $l \leqslant L$. For example, in a crystal of thickness $L_1 = 1.85 \cdot 10^{-2}$ cm, electrons which had lost $\Delta\varepsilon > 0.6\varepsilon_0$ had $x_1(l) < 4.2$, and for $L_2 = 4 \cdot 10^{-2}$ cm for the same energy loss $x_1(l) < 11$.

Thus, there is a group of electrons which at all times are close to the axis, in the region of high field strengths E. For them the intensity of radiation is appreciably enhanced, for example, at $x_1 = 2.5$ and $\varepsilon = 150$ GeV it is enhanced by seven times and the total probability of radiation by five times (for the same values of x and ε), and therefore the cascade develops more intensely. The radiation spectrum in this group is somewhat harder than for superbarrier particles, but the high loss is due not to this but to the high multiplicity of the radiation. As a result of the large value of multiple scattering and the appreciable dispersion of the distribution in ε which arises in the radiation process, the particles in this group are strongly mixed, so that as a result the distribution in x turns out to be uniform for them.[10] Although the fraction of particles belonging to this group is relatively small, nevertheless their contribution to the energy loss spectrum turns out to be extremely important for a certain interval of thicknesses.

7. INCOHERENT RADIATION AND PAIR PRODUCTION IN CRYSTALS

In addition to the determinate motion of the particles in the external field of an oriented crystal, they are scattered by potential fluctuations due to vibrations of the atoms in the crystal lattice. This scattering is accompanied by radiation, which in crystals is customarily called incoherent. In an amorphous material, where the mean field is equal to zero, radiation and pair production occur only as the result of this scattering of the particles. In oriented single crystals incoherent processes are modified in comparison with the amorphous case, mainly for two reasons.

The first reason (geometrical factors) is due to the fact that the distribution in the impact parameters of the particles taking part in the process turns out to be nonuniform in a crystal. For example, the density of the nuclei of a string is smeared in the transverse plane only as the result of thermal (and zero-point) vibrations: $n_N(\rho) = \exp(-\rho^2/2u_1^2)/2\pi u_1^2$. In addition, in the radiation problem the distribution of the incident particles in the transverse coordinate can also be nonuniform (redistribution of the flux). Under such conditions the standard theory of bremsstrahlung in which the states of the particles are described by plane waves turns out to be incorrect, and it is necessary to use the theory developed in Ref. 49. In this theory a space-time approach is used,

in which the inhomogeneity of the particle density can be taken into account in a natural way.

The second reason is the curved nature of the particle trajectory in the mean field of the axis, which in particular leads to redistribution of the charged-particle flux, and at sufficiently high energies can also directly influence bremsstrahlung processes. This influence is due to the decrease of the formation length of the processes as a result of the relatively large rotation of the particle velocity in this length and the corresponding increase of the separation angles of the final particles. This group of questions can be studied by means of the approach developed in Ref. 50 for treatment of bremsstrahlung with inclusion of effects of the medium and an external field.

We shall make a qualitative analysis of the influence of the external field on bremsstrahlung. If a photon with frequency ω is radiated by an electron (positron) with energy ε at an angle ϑ to the direction of its velocity, the formation length of this photon is determined by the relation (see for example Ref. 3)

$$l_\omega \sim \frac{(\varepsilon - \omega)\,\gamma^2}{\varepsilon\omega\,(1 + \gamma^2\theta^2)} = \frac{\gamma\lambdabar_c}{u\zeta}\,,\qquad(7.1)$$

where $u = \omega/(\varepsilon - \omega)$, $\zeta = 1 + \gamma^2\vartheta^2$. $\lambdabar_c = 1/m$. In weak fields the characteristic angles of radiation $\vartheta \sim 1/\gamma\,(\zeta \sim 1)$ and the influence of the external field can be neglected if the following condition is satisfied:

$$wl_\omega = \frac{eE}{\varepsilon}\,l_\omega \ll \frac{1}{\gamma}\,,\qquad(7.2)$$

where w is the acceleration of the particle. Substituting (7.1) into (7.2), we have a criterion of weakness of the field

$$\gamma\,\frac{eE}{\varepsilon}\,\frac{\gamma^2}{\varepsilon u} = \frac{\chi}{u} \ll 1,\qquad(7.3)$$

where the parameter $\chi(\rho)$ is defined in (3.6). Since incoherent processes occur mainly at impact distances $\rho \lesssim u_1$, where the density of the nuclei is appreciably different from zero, it is necessary to use as $\chi(\rho)$ in estimates the value $\chi_1 \approx \varepsilon V_0/m^3 u_1$ ($\varkappa_1 = \omega V_0/m^3 u_1$ for pair production).

If the condition (7.3) is satisfied, incoherent processes in crystals are changed as the result of geometrical factors, the role of which qualitatively reduces to increase of the minimum value of momentum transfer up to $q_{\min} \approx u_1^{-1}$. In the case of a uniform distribution of electrons we have for the cross section for (incoherent) bremsstrahlung[51]:

$$d\sigma_\gamma(\omega) = \frac{4Z^2\alpha^3}{m^2}\,\frac{\varepsilon - \omega}{\varepsilon}\,\frac{d\omega}{\omega}\left\{\left(\frac{\varepsilon - \omega}{\varepsilon} + \frac{\varepsilon}{\varepsilon - \omega} - \frac{2}{3}\right)\right.$$
$$\left. \times\left[\ln(183Z^{-1/3}) - g(\delta_0) - f(Z\alpha)\right] + \frac{1}{9}\right\},\quad(7.4)$$

where the function $f(Z_\alpha)$ determines the Coulomb corrections and the function $g(\delta)$ takes into account the nonuniformity of the distribution of atoms:

$$f(x) = x^2 \sum_{n=1}^{\infty} \frac{1}{n\,(n^2 + x^2)}\,,$$
$$g(\delta) = \frac{1}{2}\int_0^\infty \frac{x\,d\,xe^{-\delta x}}{(1 + x)^2}\,,\quad \delta_0 = \frac{u_1^2}{a^2}\qquad(7.5)$$

in a Moliere potential $a \approx 111Z^{-1/3}\lambdabar_c$. If the distribution of

electrons is nonuniform, but the density gradients are substantial only for $\rho \gg u_1$, the cross section (7.4) must be multiplied by a factor $n_c(0)$ ($n_c(\rho)$ is the ratio of the density of electrons to the density of a uniform distribution). The cross section for incoherent production of pairs by a photon, differential in ε, in a crystal for $\varkappa_1 y(1 - y) \ll 1$ ($y = \varepsilon/\omega$) is obtained from (7.4) by the substitutions (2.3).

When $\chi/u \gg 1$, the characteristic angles of radiation are $\vartheta \gg 1/\gamma$. The effective angle of radiation ϑ_{eff} is determined from the condition of self-consistency of its determination: the angle of deflection of a particle in a field in the formation length does not exceed ϑ_{eff} (this question has been analyzed in Ref. 50):

$$wl_\omega\,(\vartheta_{\text{eff}}) \sim \vartheta_{\text{eff}}\,,\quad \vartheta_{\text{eff}} \sim \frac{1}{\gamma}\left(\frac{\chi}{u}\right)^{1/3}\,,$$

$$\zeta \sim \left(\frac{\chi}{u}\right)^{2/3}\,,\quad l_\omega\,(\vartheta_{\text{eff}}) \sim \frac{\gamma\lambdabar_c}{u}\left(\frac{u}{\chi}\right)^{2/3}\,.\qquad(7.6)$$

We note that for $\chi/u \gg 1$ neither the characteristic radiation angle nor the photon length depend on the mass of the radiating particle.

As a result of the very high density of nuclei near an axis, where incoherent processes are important, at high electron energies the Landau-Pomeranchuk effect could appear (see for example Ref. 3). Therefore for a systematic estimate of ϑ_{eff} it is necessary to take into account in addition the broadening of the radiation angles as the result of multiple scattering. Taking into account the change of the particle deflection angle in the formation length of the photon both as the result of the external field and as the result of multiple scattering, we obtain from the condition of self-consistency

$$\frac{\chi^2}{u^2\zeta^2} + \frac{4\pi Z^2\alpha^2\gamma n}{m^3 u\zeta}\ln\frac{\zeta}{\gamma^2\vartheta_1^2} \lesssim \zeta,\qquad(7.7)$$

where Z is the charge of the nucleus, n is the density of nuclei in the medium, and $\vartheta_1 = (\varepsilon u_1)^{-1}$ is the angle corresponding to the lower limit of momentum transfers. A maximal estimate for k—the ratio of the contributions of multiple scattering and the external field to the left-hand part of Eq. (7.7)—gives[51]

$$k_{\max} \sim \frac{Z\alpha\lambdabar_c}{u_1}\ln\left(\frac{u_1}{\lambdabar_c}\right)^2 \ll 1.\qquad(7.8)$$

The condition $k \ll 1$ permits us, in calculation of the probabilities of incoherent processes, to use perturbation theory in the scattering and to neglect the Landau-Pomeranchuk effect.[51,52]

Since the photon formation length for large $\chi/u \gg 1$ falls off as $(u/\chi)^{2/3}$ the bremsstrahlung cross section falls off in the same way. For $\chi_1 \gg 1$ we have[51]:

$$\frac{d\sigma_\gamma}{d\omega} = A_\gamma\,\frac{2Z^2\alpha^3\Gamma\,(1/3)}{5m^2\omega}\left(\frac{u}{3\chi_1}\right)^{2/3}$$
$$\times\,\ln\left[mu_1\left(\frac{\chi_1}{u}\right)^{1/3}\right]\left(1 + \frac{(\varepsilon - \omega)^2}{\varepsilon^2}\right),\qquad(7.9)$$

where the constant A_γ is given by the expression

$$A_\gamma = \int d^2\rho n_e\,(\rho)\,n_N\,(\rho)\left(\frac{\chi_1}{\chi(\varrho)}\right)^{2/3}\,.\qquad(7.10)$$

In the potential (3.7) we find $A_\gamma \approx 1.5n_e(0)$. The cross sec-

tion for incoherent pair production for $x_1 \gg 1$ $(\omega \gg \omega_h)$, (3.12), is obtained from (7.9) by the replacements (2.3), and the corresponding constant A_c is given by Eq. (7.10), in which it is necessary to make the substitution $n_e(\rho) \to 1$.

The cross section (7.9) was obtained with logarithmic accuracy. The argument of the logarithm in (7.9) is the ratio q_{max}/q_{min}, and in accordance with (7.6) an increase of the maximum momentum transfer has occurred: $q_{max} \to m(\chi_1/u)^{1/3}$.

The relative magnitude of the contribution of incoherent processes to radiation and pair production in crystals in comparison with effects in the averaged field of axes falls off with increase of the energy. It is small already in the region where $L_{ch}^{-1}(\varepsilon)$ and $W_e(\omega)$ reach their maximum value $(r_\gamma^{max}, r_e^{max} \gg 1)$, and continues to decrease with further increase of the energy. For example, integrating (7.9) over $d\omega$ with a weight ω and multiplying the result by N—the average density of atoms in the crystal, we obtain with logarithmic accuracy the intensity of incoherent radiation

$$\frac{I^{nc}}{\varepsilon} = \frac{8 \cdot 29 \pi N}{5 \cdot 3^5 3^{1/6}} \Gamma\left(\frac{1}{3}\right) A_\gamma \frac{Z^2 \alpha^3}{m^2 \chi_1^{2/3}} \ln(mu_1 \chi_1^{1/3}). \quad (7.11)$$

Then for the ratio of the intensity I^{nc} to the intensity of radiation in the field of the axis I^F ($\chi_s \gg 1$, and potential (3.7) is used) we have[51]

$$\frac{I^{nc}}{I^F} \lesssim 10^{-2} \frac{Z\alpha}{\chi_1^{1/3}} \frac{\ln(mu_1 \chi_1^{1/3})}{\ln \chi_s} \ll 1. \quad (7.12)$$

Exactly the same estimate is obtained for $x_s \gg 1$ for the ratio of the probability of incoherent pair production to the probability of the process in the field of an axis.

8. COMPARISON OF THEORY WITH EXPERIMENT

At the present time two experimental groups, I (France, USA) and II (Denmark, Great Britain, France), are carrying out experimental studies of pair production and radiation in crystals, using the SPS accelerator at CERN, in which there are beams of electrons (positrons) and photons with energy up to 150 GeV. We shall compare the results of the experiment with the theory given above.

8.1. Pair production. In Refs. 28, 30, 32, and 33 the dependence of the total probability of pair production on the photon energy ω and the orientation dependence $W_e(\vartheta_0)$ were measured for several intervals of ω in single crystals of Ge oriented near the $\langle 110 \rangle$ axis at $T \approx 100$ K. In this situation $\omega_1 = 50$ GeV, and a rearrangement of the picture of the orientation dependence due to change of sign of the correction for $\vartheta_0 \ll \vartheta_V$ occurs (see Fig. 6) at $\omega_1 \approx 230$ GeV.

The result of a theoretical calculation of the function $W_e^F(\omega)$ for the experimental conditions was given in Ref. 13. In Fig. 11 this same curve is shown with addition of a modified incoherent contribution[11] $W_{BH}^M = 0.28$ cm^{-1}, whereas $W_{BH} = 0.32$ cm^{-1}. The experimental points have been taken from Refs. 32 and 33. Good agreement between theory and experiment can be seen.

In Fig. 12 we have given curves of the orientation dependence calculated on the basis of Refs. 14 and 15 (see Fig. 7) and in addition averaged over energy intervals in accordance with the conditions of Ref. 32. In Fig. 13 we have shown the results of a similar procedure under the conditions of the experiment of Ref. 33. The experimental data
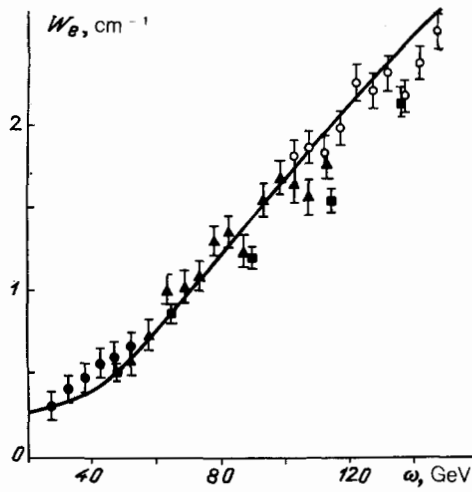

FIG. 11. Total probability of pair production in Ge $\langle 110 \rangle$ ($T = 100$ K) as a function of energy. The experimental data are from Ref. 32 (except the squares), the squares are from Ref. 33, and the theoretical curve is from Refs. 13–15.

confirm all qualitative features of the theoretical description developed. For example, in Figs. 12 and 13 we can easily see a shift to the left with increasing energy of the maximum of the curve $W_e(\vartheta_0)$ and a narrowing of the maximum, which is due to the more rapid rise with energy of the pair production probability in the field of an axis in comparison with coherent pair production. In regard to the quantitative agreement of the theory and experiment, for all energy intervals the accuracy of the agreement has turned out to be better than 20%. Improvement of the theoretical predictions can be achieved by removing adjustable fit procedures from the calculation (for the potential of the axis, for the orientation curve at $\vartheta_0 \sim \vartheta_V$). It is also necessary to improve further
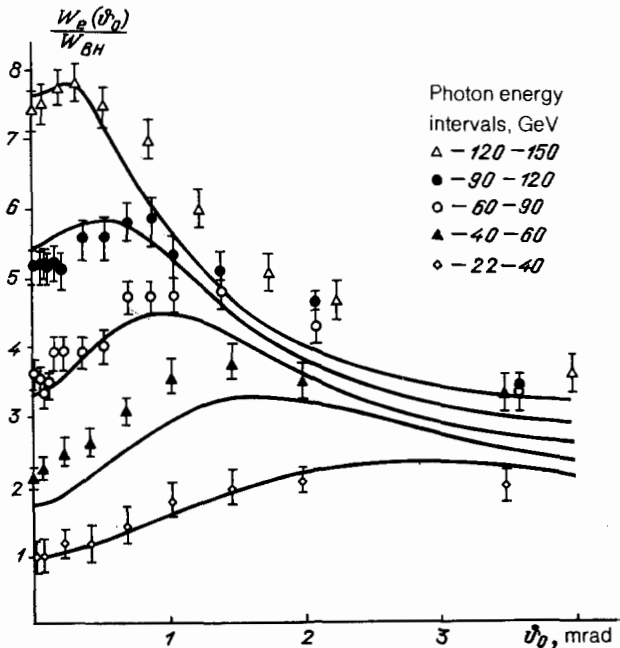

FIG. 12. Orientation dependence of the total probability of pair production in Ge $\langle 110 \rangle$ ($T = 100$ K) for photons with energy in the energy intervals indicated. The experimental data are from Ref. 32.

Photon energy intervals, GeV
△ — 120 −150
● — 90 − 120
○ — 60 − 90
▲ — 40 − 60
◇ — 22 − 40

W_e / W_{BH}

(1) ● $-40-50$ GeV
(2) ■ $-50-75$
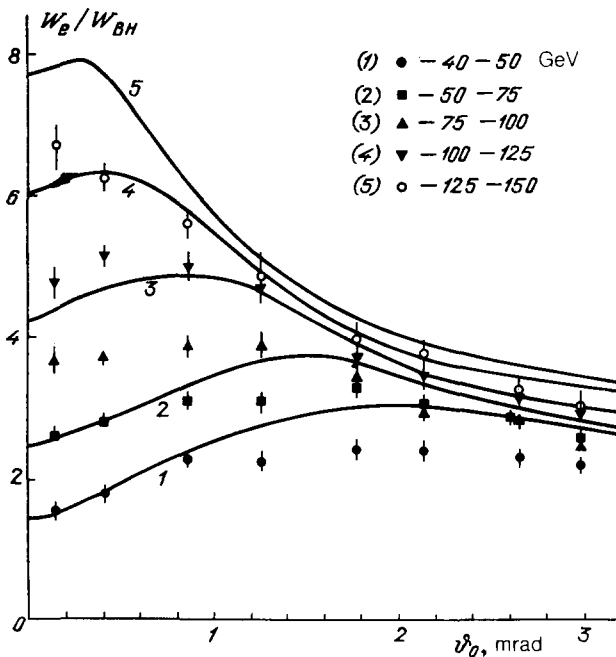(3) ▲ $-75-100$
(4) ▼ $-100-125$
(5) ○ $-125-150$

FIG. 13. The same as Fig. 12 but for other photon energy intervals (data of Ref. 33).

the experimental data, since there is a small difference in the results of the experiments of Refs. 32 and 33, which were carried out under identical conditions.

8.2. Radiation. The average energy loss was calculated for a uniform distribution in Ref. 18 and is in good agreement with the data of the experiment of Refs. 29 and 30. The approach developed in Ref. 18 permitted treatment in Ref. 11 also of the orientation dependence of the average energy loss. The result of the calculation and the experimental data from Refs. 29 and 30 are shown in Fig. 14. The crystal used in the experiment with $L = 0.14$ cm is already rather thick (see the discussion in Section 6) for electrons, and therefore we assumed for them that $F(\rho, \vartheta_0) = 1$, i.e., the distribution was considered uniform for all angles of incidence ϑ_0. On the contrary, for positrons in the first approximation multiple scattering can be neglected, and a calculation was carried
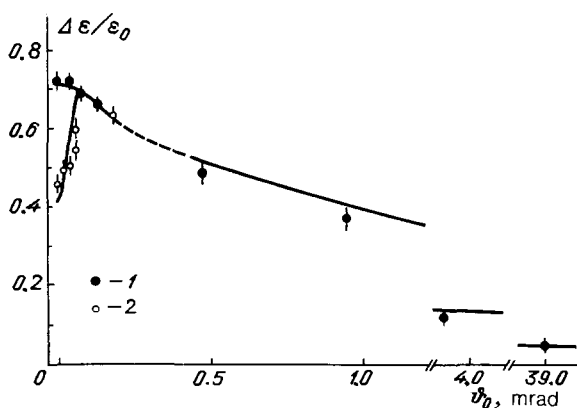

$\Delta\varepsilon/\varepsilon_0$

● -1
○ -2

ϑ_0, mrad

FIG. 14. Relative energy loss as a function of entry angle with respect to the ⟨110⟩ axis of a Ge crystal ($T = 100$ K, initial energy $\varepsilon_0 = 150$ GeV, $L = 1.4$ mm). The numbers of the curves have the same meaning as in Fig. 8. The experimental data have been taken from Refs. 29 and 30: 1—electrons, 2—positrons.

out as for a thin crystal with inclusion of the effective angular width of the incident beam.

In addition to the average loss, the spectral distributions were also measured. However, since the detectors used measured only the combined energy of the photons radiated by a particle

$$\Delta\varepsilon = \sum_n \omega_n^j,$$

we actually observed not the true photon spectra, but the distributions in the energy loss $\Delta\varepsilon$. Under conditions of high multiplicity these two distributions will be completely different. Therefore the peak in the loss spectrum which was observed in a recent experiment[31] carried out using a comparatively thin crystal with $L = 1.85.10^{-2}$ cm, which has attracted universal attention, does not signify appearance of a previously unknown mechanism of hard radiation. This effect can be described in the framework of the approach developed above if one takes into account the cascade nature of the process and the influence of the radiation on its kinetics.

On the basis of the treatment given at the end of Section 6, the following simple model of the phenomenon was proposed in Ref. 35. We divide the particles into two groups on the basis of the initial population: the first, for which x_1 (0) $< x_b < x_0$, and the second which includes all remaining particles, both those which have been captured into a channel and superbarrier particles. It was further assumed that in the entire thickness of the crystal the particles of the first group have a uniform distribution in the coordinate with some value $x_1 = x_{\text{eff}} < x_b$, while the distribution of the remaining particles is the same as for the superbarrier particles. After this, with the particle distribution now known, it is possible to calculate for each group the characteristics of the cascade. The value of x_b can be estimated by using the solution of the system of equations (6.7) and the dispersion which arises in the distributions in $\varepsilon_\perp$ and ε; however, strictly speaking, in the framework of the description developed x_b, like x_{eff}, are adjustable parameters. With increase of the thickness of the crystal the values of x_b and x_{eff} increase and, when x_b reaches values x_0 (for the conditions under discussion this occurs at $L \approx 8 \cdot 10^{-2}$ cm), the particles of the second group overtake those of the first group in energy loss and the contribution of the first group to the spectral distribution in $\Delta\varepsilon$ can no longer be separated; therefore for $L = 0.14$ cm it is sufficient to consider the radiation of one group of particles. It must be kept in mind that the number of particles in the first group is always small. For example, at $\vartheta_0 = 0$ and $\Delta\vartheta_0 = 30$ μrad only 19% of the particles are captured into the channel initially and still fewer particles have a value x_1 (0) $< x_b$. For sufficiently small thicknesses the peak in the spectral distribution in $\Delta\varepsilon$ due to the particles of the first group also drops out as the result of the decrease with crystal thickness of the number of particles in this group (x_b decreases) and, mainly, as a result of decrease of the multiplicity of radiation. Under the conditions of Ref. 31 this should occur at $L \approx (5-7.5) \cdot 10^{-3}$ cm. With increase of the energy for a fixed thickness of the crystal the value of x_b will decrease, and for superbarrier particles radiative capture of them into a channel can become important.

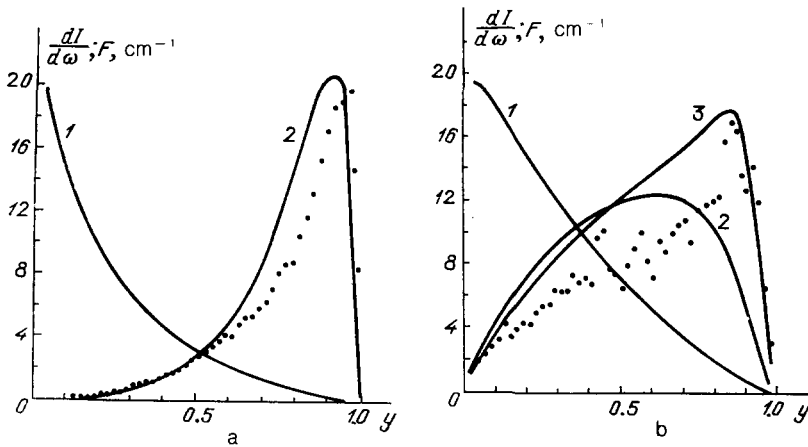Turning to comparison of the theoretical and experi-

FIG. 15. Spectral distribution in Ge ⟨110⟩ (T = 100 K) in the form given by Eq. (8.1). (a)—For a thickness $L = 1.4$ mm; curve 1—true photon spectrum, curve 2—energy loss spectrum. (b)—For a thickness $L = 0.4$ mm; curve 1—true spectrum, curve 2—for a uniform distribution, curve 3—with inclusion of the contribution of particles of the first group.

mental values, we recall that the distribution in the energy loss $y = \Delta\varepsilon/\varepsilon_0$ was measured. We shall also give the calculated true spectrum of radiated photons, which as the result of the high multiplicity differs appreciably from the loss spectrum. In this case the quantity y will denote the ratio ω/ε, where ω is the photon frequency. Let us consider the quantity

$$F = \frac{a}{\cdot L}\, y\, \frac{dN_1}{dy} + \frac{(1-a)}{\cdot L}\, y\, \frac{dN_2}{dy}, \qquad (8.1)$$

where, in accordance with the model used, a is the number of particles falling in the first group (subscript 1). For $L = 0.14$ cm, as was explained above, it is necessary to set $a = 0$. The distribution dN_2/dy was found in Ref. 27, where we have given the distribution of particles in energy, which differs from dN_2/dy only in the replacement $y \rightarrow 1 - y$. In Fig. 15a we have given these results and the data of the experiment of Refs. 29 and 30 in the form (8.1). We can see the satisfactory agreement of the theoretical and experimental values[12] and the striking difference of the true photon spectrum (curve 1) from the energy loss spectrum (curve 2), which is due to the high multiplicity (see the discussion in Section 6).

For $L = 0.04$ cm we took $x_c = 11$ and $x_{eff} \approx 6$. Then for $\vartheta_0 = 0$ for a beam divergence $\Delta\vartheta_0 = 30$ μrad we find $a \approx 0.15$. In order to demonstrate the contribution of the particles of the first group, in Fig. 15b we have plotted the quan-

tity F for $a = 0$ (curve 2) and for $a = 0.15$ (curve 3), and also the true spectrum for $a = 0$ (curve 1). The experimental data from Ref. 30, which are also shown in Fig. 15b, favor the existence of particles of the first group. There is some discrepancy in the absolute values. This may be due to the fact that the normalization of the curve for $L = 0.04$ cm in Fig. 2 of Ref. 30 differs appreciably from unity.

For $L = 1.85 \cdot 10^{-2}$ cm we chose $x_b = 4.2$ and $x_{eff} = 2.5$. Then for $\vartheta_0 = 0$ ($\Delta\vartheta_0 = 30$ μrad) we obtained $a = 0.087$, and for $\vartheta_0 = 17$ μrad we obtained $a = 0.073$. Unfortunately the spectral distributions in Fig. 3 of Ref. 31 were given without subtraction of the background. Therefore we have compared the difference of the experimental values for $\vartheta_0 = 0$ and $\vartheta_0 = 96$ μrad, on the one hand, and $\vartheta_0 = 17$ μrad and $\vartheta_0 = 96$ μrad respectively. Since for $\vartheta_0 = 96$ μrad even with allowance for the divergence of the initial beam all particles are initially superbarrier ($a = 0$), this difference in our model is given by the expression

$$\Delta F = \frac{ay}{L}\left(\frac{dN_1}{dy} - \frac{dN_2}{dy}\right). \qquad (8.2)$$

This quantity for $\vartheta_0 = 0$ is plotted in Fig. 16a (curve 2), and for $\vartheta_0 = 17$ μrad it is plotted in Fig. 16b. The calculation agrees quite well with experiment. In this way the adequacy of the model proposed for the kinetics is confirmed. The very existence of the peak[13] in the distribution in $\Delta\varepsilon$ is due to the high multiplicity of the radiation of the particles of the first
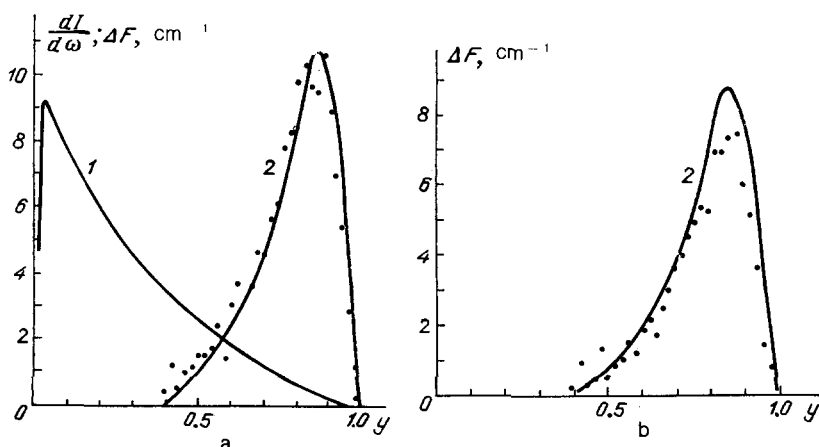

FIG. 16. Spectral distribution in Ge ⟨110⟩ ($T = 100$ K) for $L = 0.185$ mm in the form of Eq. (8.2). (a)—For an angle of entry $\vartheta_0 = 0$; curve 1—true spectrum, curve 2—loss spectrum. (b)—For an entry angle $\vartheta_0 = 17$ μrad, only curve 2. (Data of Ref. 31).
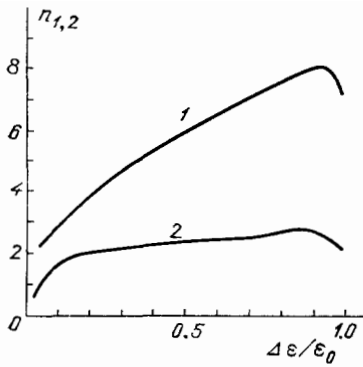
FIG. 17. Multiplicity of photons as a function of energy loss. Curves 1 and 2 are the contributions of particles of the first and second groups respectively.

group. This is clear from comparison of this spectrum with the true spectrum of photons from this group (curve 1 in Fig. 16a) and is further illustrated by Fig. 17, where we have shown the results of calculation of the dependence of the multiplicity (for $\omega > 1$ GeV, in accordance with the conditions of the experiment of Ref. 31) on the energy loss for particles of the first group, n_1 (curve 1), and of the second group, n_2 (curve 2), for $L = 1.85 \cdot 10^{-2}$ cm. Experimentally one should observe a multiplicity distribution $n = an_1 + (1 - a)n_2$. Substituting for the experiment of Ref. 31 $a = 0.087$, for $\vartheta_0 = 0$ we have in the interval $0.82 < y < 0.9 n = 3.2$. In a recent study by Belkacem et al.[55] the authors of the experiment indirectly (by measurement of the probability of conversion of photons into pairs) extracted the multiplicity of photons. In this interval and for an effective cutoff in radiated photon energy $\omega_{\rm eff} \simeq 100$ MeV it is $n = 3.8$ or $n = 4.3$ (depending on the method of analysis).
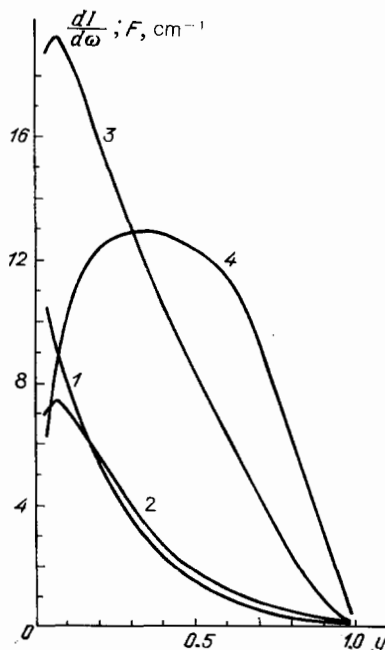

FIG. 18. Spectral distributions of intensity in the form of Eq. (8.1); $L = 0.185$ mm. True photon spectra: curve 1—for positrons with $\vartheta_0 = 0$, curve 3—for positrons and electrons with $\vartheta_0 = 96\,\mu$rad. The distribution in loss under the same conditions—curves 2 and 4 respectively.

For these conditions ($\omega > \omega_{\rm eff}$) our prediction is $n = 3.7$. In Ref. 55 a comparison is made with Refs. 53 and 54, and it is stated that the observed multiplicity is much less than the predictions of Ref. 53 ($n \approx 12$) and Ref. 54 (n somewhat less than 12). In Fig. 18 we have shown the results on the spectral distribution of the energy loss and the true photon spectrum for $\vartheta_0 = 96\,\mu$rad, when the electrons and positrons should radiate identically (curves 4 and 3). As has already been mentioned, for positrons at $\vartheta_0 = 0$ a crystal with $L = 1.85 \cdot 10^{-2}$ cm is thin, and the calculation (curves 2 and 1 in Fig. 18) was carried out with the initial distribution of particles. As the result of redistribution of the flux, the radiation of positrons with $\vartheta_0 = 0$ is appreciably weaker than for superbarrier particles.

Thus, our analysis shows that the theory quite satisfactorily describes the entire set of experimental data on pair production by a photon and on radiation from particles in oriented crystals.

9. PROCESSES OF HIGHER ORDER AND PROCESSES INVOLVING OTHER PARTICLES

We have discussed above the principal processes of lower order—radiation by an electron (positron) and production of an electron-positron pair by a photon. Naturally, they have the greatest probabilities. In addition to them other processes can occur. We shall discuss some of them.

9.1. Production of a pair by a charged particle ($e^{\pm} \rightarrow e^{\pm} e^- e^+$).
This process, which occurs by means of a virtual photon (v), and which we shall call direct electroproduction, in its properties (spectra, angular distributions) is similar to the successive process $e^{\pm} \rightarrow e^{\pm} \gamma$, $\gamma \rightarrow e^+ e^-$ which was taken into account in discussion of the cascade. Therefore for experimental separation of direct electroproduction it is necessary to find conditions under which its probability exceeds the probability of the successive process. For definiteness we shall consider this question under the conditions of the experiment of Ref. 30. In this case for estimation of the number of charged particles produced in the successive process $N_e (L)$ one can directly use Eq. (6.6) and, since small thicknesses will be considered, we can neglect the change of energy of the initial particle. We have from (6.6)

$$N_e(L) \approx 30L^2, \qquad (9.1)$$

where L is in centimeters. The number of particles produced in the direct electroproduction process will be $N_v (L) = 2W_v L$, where the probability W_v must be taken at $\varepsilon = 150$ GeV. An estimate of W_v in the region considered $\chi \sim 1$ can be obtained on the basis of Refs. 56 and 57 on electroproduction of pairs in an external field:

$$N_v (L) \approx \frac{L}{5}. \qquad (9.2)$$

It follows from this that N_e and N_v become equal at a thickness $L = 70\,\mu$m. Since it is possible to use even thinner crystals, it is clear that the direct electroproduction process can be separated experimentally already now. Since $N_e/N_v \sim L$, with decrease of the thickness its separation is improved. However, L cannot be taken less than the formation length of the process. At a high energy ($\chi \gg 1$) when the virtuality of the photon is small, this length coincides with the ordinary formation length of radiation l_f (see Section 3). For example, for the $\langle 110 \rangle$ axis of Ge at $\varepsilon = 100$ TeV, when l_f

$\approx 10^{-3}$ cm, we have for $L = l_f$ the maximum ratio N_v / N_c ≈ 120, i.e., under these conditions direct electroproduction is dominant.

9.2. Splitting up of a photon ($\gamma \to \gamma\gamma$). The process occurs through an electron-positron loop in the field of a crystal. This process was studied in detail in Refs. 58 and 59. Here also there is an enhancement of the effect in the field of an axis in comparison with the process at an isolated nucleus. However, observation of the process of photon splitting up (which incidentally has not been observed up to the present time) is an extremely complicated problem, since the ratio of the probabilities is

$$\frac{W^F_{\gamma \to \gamma\gamma}}{W_{\gamma \to e^+e^-}} \approx 0.3 \, \frac{\alpha^2}{\pi^2} . \tag{9.3}$$

9.3. Production of a neutrino pair by an electron ($e \to 2\nu\bar{\nu}$). This process in an external field was discussed in Ref. 60. In the field of a crystal it is necessary to carry out an appropriate averaging of the probabilities. As a result we have, for example, for the case $\chi_s \gg 1$

$$\frac{W^F_{e \to e\nu\bar{\nu}}}{W^F_{e \to e\gamma}} \simeq 4 \cdot 10^{-4} \frac{G^2 m^4}{\alpha} \chi_s^{4/3} \left[(1+2\eta) \ln \frac{1+\eta}{\eta} - 2 \right], \tag{9.4}$$

where G is the weak interaction constant. The combination of constants entering into this formula is very small ($G^2 m^4 \alpha \sim 10^{-21}$) which essentially excludes (now and in the foreseeable future) crystals from candidates for generation of neutrinos (see however Ref. 61).

9.4. Production of a π^0 meson by a photon ($\gamma + \gamma$ in the field of a crystal $\to \pi^0$). Production of a π^0 by a photon in a Coulomb field (the Primakoff effect) is used for determination of the lifetime τ_π of this meson. In a crystal (cf. Ref. 62) a similar coherent effect is possible.

If we neglect that τ_π is finite (the corresponding decay width of the π^0 is $\Gamma \approx 7.6$ eV), then in a two-photon process the conservation law $Q + k = p_\pi$ must be satisfied, or

$$2\omega |q_{\parallel}| = \mu^2, \tag{9.5}$$

where μ is the mass of the π^0 meson. We recall that $q_{\parallel} = \mathbf{q}\mathbf{v} = \mathbf{q}_\perp \mathbf{v} + q_n \cos\vartheta_0$, $\mathbf{v} = \mathbf{k}/\omega$, and $q_n = (2\pi/d)n_z$, where n_z is an arbitrary integer. We shall assume that $\vartheta_0 \ll 1$, and in that case $q_{\parallel} \approx q_n + \mathbf{q}_\perp \cdot \mathbf{v}$ and $\mathbf{q}_\perp \mathbf{v} \sim |\mathbf{q}|\vartheta_0 \ll |q_n|$ for $n_z \neq 0$. Since in a crystal values of $|q_{\parallel}|$ are limited on the high side by the existence of the factor $\exp(-\mathbf{q}^2 u_1^2)$ (see Eq. (2.12)), we obtain from (9.5) an estimate for the threshold frequency of the photon $\omega_{th} \approx \mu^2 u_1 /2$. For example, in diamond at room temperature $\omega_{th} \approx 200$ GeV. We note that for $n_z = 0$ this threshold lies inaccessibly high, i.e., in contrast to the coherent processes discussed in Section 4, the term with $n_z = 0$ has no effect. We can analyze the effect in terms of equivalent photons, writing its probability in the same way as in Eq. (4.8):

$$W^{coh}_{\gamma \to \pi^0} = \sum_q \frac{|G(\mathbf{q})|^2 \mathbf{q}_\perp^2}{4\pi\alpha |q_{\parallel}|} \sigma_{\gamma\gamma} (|q_{\parallel}|, \omega), \tag{9.6}$$

$$W^{nc}_{\gamma \to \pi^0} = \frac{Z^2 \alpha N}{2\pi^2} \int \frac{d^2 q_\perp \mathbf{q}_\perp^2}{(\mathbf{q}^2 + a^{-2})^2} \frac{dq_{\parallel}}{|q_{\parallel}|} \sigma_{\gamma\gamma} (|q_{\parallel}|, \omega).$$

In (9.6) we made use of the expression for the flux (1.5) and gave also the probability of the similar incoherent process

$W^{nc}_{\gamma \to \pi^0}$, where N is the average density of atoms and a is the corresponding screening radius. The cross section for production of a π^0 meson by two photons $\sigma_{\gamma\gamma} (|q_{\parallel}|, \omega)$ has the form of a Breit-Wigner resonance distribution:

$$\sigma_{\gamma\gamma} (|q_{\parallel}|, \omega) = \frac{8\pi\Gamma^2}{(2\omega |q_{\parallel}| - \mu^2)^2 + \Gamma^2 \mu^2} . \tag{9.7}$$

The coherent Primakoff effect, as a result of the discreteness of the equivalent photon spectrum (of the values of $q_{\parallel}$), occurs only for certain frequencies $\omega_n = \mu^2/2|q_n|$. If the angular and energy spreads in the incident beam of photons satisfy the condition $\Delta\vartheta_0, \Delta\omega/\omega \lesssim \Gamma/\mu$, then the probability $W^{coh}_{\gamma \to \pi^0}$ will not depend on the width Γ and will significantly exceed the value of $W^{nc}_{\gamma \to \pi^0}$. However, since $\Gamma/\mu < 6\cdot 10^{-8}$, the inverse equality is actually realized: $\Delta\vartheta_0, \Delta\omega/\omega \gg \Gamma/\mu$, and usually $\Delta\omega/\omega \gg \Delta\vartheta_0$ and $\Delta\omega \ll \omega_n - \omega_{n \pm 1}$. Under these assumptions and for a uniform distribution, averaging (9.6) over frequency in an interval $\Delta\omega$ near ω_n, we find

$$\langle W^{coh}_{\gamma \to \pi^0} \rangle \approx \frac{2\pi\Gamma}{\alpha\mu^3} \left(\frac{\omega_n}{\Delta\omega} \right) \frac{1}{|q_n|} \sum_{\mathbf{q}_\perp} |G(\mathbf{q}_\perp, q_{\parallel} = q_n)|^2 \mathbf{q}_\perp^2,$$

$$\langle W^{nc}_{\gamma \to \pi^0} \rangle \approx \frac{8\pi Z^2 \alpha\Gamma}{\mu^3} N \int_{(q_\perp^{min})^2}^{(q_\perp^{max})^2} \frac{x \, dx}{(x + q_n^2 + a^{-2})^2} . \tag{9.8}$$

For a threshold energy $\omega_n \approx \omega_{th}$, setting in (9.8) $|q_n| \approx u_1^{-1}$ and replacing the summation $\Sigma_{\mathbf{q}_\parallel}$ by an integral, we obtain a rough estimate for the ratio of the coherent and incoherent effects:

$$\frac{\langle W^{coh}_{\gamma \to \pi^0} \rangle}{\langle W^{nc}_{\gamma \to \pi^0} \rangle} \sim \frac{\omega_n}{\Delta\omega} \frac{u_1}{l}, \quad \omega \approx \omega_{th}, \tag{9.9}$$

where l is the lattice constant [see (2.9)]. It can be seen that the enhancement factor which arises as the result of the discreteness of the spectrum ($\omega_n /\Delta\omega$) turns out to be compensated to a significant degree. For example, in diamond $u_1 /l \sim 10^{-2}$. Nevertheless for a photon beam with $\Delta\omega/\omega \lesssim 10^{-2}$ observation of the coherent effect is already possible at the present time. This conclusion was drawn in Ref. 62.

10. CONCLUSION

Thus, in the eighties our knowledge of the principal electromagnetic processes in crystals has expanded significantly. It has been found that, depending on the angle of incidence of the initial particle, various mechanisms of radiation and pair production are important. In the high-energy region processes in the fields of axes (planes) occur significantly more intensely than in an amorphous medium, being a very effective mechanism of pumping of the energy of charged particles into photons and of photons into electron-positron pairs.

These features of the processes may find practical application. One of the applications is in small-size converters which turn the energy of charged particles into radiation. A second possible application is use of crystals for detection of photons, electrons, and positrons[63,48] (the suggestion of use of radiation in channeling in astrophysical detectors was made in Ref. 64). From our analysis it follows that with use of crystals it is possible to create a comparatively compact

electromagnetic calorimeter which has in addition high angular resolution. These two qualities may be useful both in high energy physics and in astrophysics. In the low-energy region (tens of MeV), where the mechanism of electron radiation is completely different, application of the radiation process to investigation of the properties of crystals has been discussed recently in Ref. 65.

---

[1] In this article we use the system of units $\hbar = c = 1$.

[2] In addition to the mechanism discussed in a crystal there is also another mechanism of radiation and pair production due to interaction with fluctuations of the potential. For a complete description this (incoherent) distribution must be added to (2.6) and (2.8). At high energies the contribution of incoherent processes usually turns out to be small. This question is discussed below.

[3] Keeping the terms with q_z, $q_z' \neq 0$ corresponds to inclusion of the discreteness of the string of atoms forming a crystal axis. Calculation of this contribution is similar to the calculation for $\vartheta_0 \gg V_0/m$ (see Section 4).

[4] Radiation in crystals in the synchrotron-radiation limit has been discussed in Refs. 4, 5, 38, and 39, and in Ref. 5 corrections $\sim \rho^{-1}$ were obtained for the specific form of the transverse motion.

[5] The maximum electric field of the $\langle 111 \rangle$ axis in tungsten at $T = 293$ K is $5 \cdot 10^{11}$ V/cm. In silicon and diamond the fields are approximately an order of magnitude weaker.

[6] As a result of the specific behavior of the potential (3.7), due to the fact that the field strength at large distances falls off as $1/\rho^3$ the value of c_1 varies only weakly in the region of energies in which $1 \ll \chi_S \lesssim x_0^{1/2}$.

[7] It is necessary to keep in mind and to evaluate in specific situations the possibility of increase of the role of multiple scattering and change of the direction of motion in comparison with the initial direction in very large thicknesses as the result of the significant decrease of the average energy of the particles.

[8] Showers in the coherent region have also been discussed; see Ref. 43 and references cited therein.

[9] Numerical calculation of the cascade[27] gave for the number of photons with $\omega > \omega_f = 100$ MeV $N_\gamma(0.14) \approx 13.9$ and $N_\gamma(0.04) \approx 3.9$, and for the total number of photons $N_\gamma(0.14) \approx 17.3$ and $N_\gamma(0.04) \approx 4.4$, which is in good agreement with the estimates given; the same agreement exists for the number of secondary charged particles.

[10] The distribution is uniform, but not the same as for super-barrier particles, since it is concentrated in a limited region around the axis.

[11] This modification is determined by the term $g(\delta_0)$ in Eq. (7.4) if we go over to pair production by means of the substitution rules.

[12] We note that in Fig. III–15 of Ref. 34 the location of the peak (for $L = 0.14$ cm) coincides with the theoretical location in Fig. 15a.

[13] An attempt to explain the location of the peak for crystals of thickness $L = 1.85 \cdot 10^{-2}$ cm on the basis of an analysis of the average loss was made in Ref. 53, and in Ref. 54 the peak was studied by means of Monte Carlo modeling. We emphasize that the approach set forth above differs substantially from those used in Refs. 53 and 54.

---

[1] M. L. Ter-Mikaélyan, *Influence of the Medium on Electromagnetic Processes at High Energies* (in Russian), Publishing House of the Armenian Academy of Sciences, Erevan, 1969.

[2] C. Diambrini-Palazzi, Rev. Mod. Phys. **40**, 611 (1968).

[3] V. N. Baĭer, V. M. Katkov, and V. S. Fadin, *Radiation from Relativistic Electrons* (in Russian), Atomizdat, Moscow, 1973.

[4] V. N. Baĭer, V. M. Katkov, and V. M. Strakhovenko, *Radiation by Relativistic Electrons in Planar Channeling* (in Russian), Preprint 80–03, Institute of Nuclear Physics, Siberian Division, USSR Academy of Sciences, Novosibirsk, 1980.

[5] V. N. Baĭer, V. M. Katkov, and V. M. Strakhovenko, Zh. Eksp. Teor. Fiz. **80**, 1348 (1981) [Sov. Phys. JETP **53**, 688 (1981)].

[6] N. P. Kalashinkov, *Coherent Interactions of Charged Particles in Single Crystals* (in Russian), Atomizdat, Moscow, 1981.

[7] A. I. Akhiezer, V. F. Boldyshev, and N. F. Shul'ga, Fiz. Elem. Chastits At. Yadra **10**, 51 (1979) [Sov. J. Part. Nucl. **10**, 19 (1979)].

[8] V. B. Berestetskiĭ, E. M. Lifshitz, and L. P. Pitaevskiĭ, *Quantum Electrodynamics*, 2nd ed. Pergamon Press, Oxford, 1982, Russ. original, Nauka, M; 1981.]

[9] V. N. Baĭer, V. M. Katkov, A. I. Mil'shteĭn, and V. M. Strakhovenko, Zh. Eksp. Teor. Fiz. **69**, 783 (1975) [Sov. Phys. JETP **42**, 400 (1975)].

[10] V. I. Ritus and A. I. Nikishov, *Quantum Electrodynamics of Phenomena in Intense Fields* Tr. Fiz. Inst. Akad. Nauk SSSR, T. 111, 1979. Proc. (Tr.) P. N. Lebedev Phys. Inst. Vol. 111, 1979.

[11] V. N. Baĭer, V. M. Katkov, and V. M. Strakhovenko, Phys. Lett. **117A**, 251 (1986).

[12] V. N. Baĭer, V. M. Katkov, and V. M. Strakhovenko, Zh. Eksp. Teor. Fiz. **92**, 1228 (1987) [Sov. Phys. JETP **65**, 686 (1987)].

[13] V. N. Baĭr, V. M. Katkov, and V. M. Strakhovenko, Phys. Lett. **109A**, 179 (1985).

[14] V. N. Baĭer, V. M. Katkov, V. M. Strakhovenko, Zh. Eksp. Teor. Fiz. **90**, 801 (1986) [Sov. Phys. JETP **63**, 467 (1986)].

[15] V. N. Baĭer, V. M. Katkov, and V. M. Strakhovenko, Nucl. Instrum. Methods B **16**, 5 (1986).

[16] V. N. Baĭer, V. M. Katkov, and V. M. Strakhovenko, Dokl. Akad. Nauk. SSSR **289**, 75 (1986) [Sov. Phys. Dokl.**31**, 552 (1986)]

[17] V. N. Baĭer, V. M. Katkov, and V. M. Strakhovenko, Phys. Lett. **104A**, 231 (1984).

[18] V. N. Baĭer, V. M. Katkov, and V. M. Strakhovenko, *ibid.* **114A**, 511 (1986).

[19] V. N. Baĭer, V. M. Katkov, and V. M. Strakhovenko, Dokl. Akad. Nauk SSSR **282**, 851 (1985) [Sov. Phys. Dokl. **30**, 474 (1985).

[20] J. C. Kimball and N. Cue, Phys. Rep. **125**, 69 (1985).

[21] A. Belkacem, N. Cue, and J. C. Kimball, Phys. Lett. **111A**, 86 (1985).

[22] J. C. Kimball, N. Cue, and A. Belkacem, Nucl. Instrum. Methods B **13**, 1 (1986).

[23] V. G. Baryshevskiĭ and V. V. Tichomirov, Phys. Lett. **113A**, 335 (1985).

[24] V. G. Baryshevskiĭ and V. V. Tikhomirov, Yad. Fiz. **36**, 697 (1982) [Sov. J. Nucl. Phys. **36**, 408 (1982)].

[25] V. G. Baryshevskiĭ and V. V. Tikhomirov, Zh. Eksp. Fiz. **85**, 232 (1983) [Sov. Phys. JETP **58**, 135 (1983)]

[26] J. C. Kimball, N. Cue, L. M. Roth, and B. B. Marsh, Phys. Rev. Lett. **50**, 950 (1983).

[27] V. N. Baĭer, V. M. Katkov, and V. M. Strakhovenko, Nucl. Instrum. Methods, B **27**, 360 (1087).

[28] A. Belkacem, G. Bologna, M. Chevallier, *et al.*, Phys. Rev. Lett. **53**, 2371 (1984); **54**, 852 (E) (1985).

[29] A. Belkacem, M. Chevallier, *et al.*, *ibid.*, p. 2667.

[30] A. Belkacem, G. Bologna, M. Chevallier, *et al.*, Nucl. Instrum. Methods **B13**, 9 (1986).

[31] A. Belkacem, G. Bologna, M. Chevallier, *et al.*, Phys. Lett. **117B**, 211 (1986).

[32] A. Belkacem, G. Bologna, M. Chevallier, *et al.*, Phys. Rev. Lett. **58**, 1196 (1987).

[33] J. F. Bak, D. Barbenis, T. J. Brodbeck, *et al.*, Phys. Lett. **202B**, 615 (1988).

[34] A. Belkacem, These Docteures, Science Physique, Université de Lyon I, 1986.

[35] V. N. Baĭer, V. M. Katkov, and V. M. Strakhovenko, *Pair Production and Radiation in Oriented Single Crystals: Status of Theory and Experiment*, Preprint INP 88–17, Novosibirsk, 1988; Phys. Lett. **132A**, 211 (1988); Nucl. Instrum. Methods **B34**, 521 (1988).

[36] V. N. Baĭer, V. M. Katkov, and V. M. Strakhovenko, Dokl. Akad. Nauk SSSR **275**, 1369 (1984) [Sov. Phys. Dokl. **29**, 306 (1984); *Radiation in Motion of High Energy Particles near Crystal Axes in Thick Crystals* (in Russian), Preprint No. 83–70, Institute of Nuclear Physics, Siberian Division, USSR Academy of Sciences, Novosibirsk, 1983.

[37] V. N. Baĭer, V. M. Katkov, and V. M. Strakhovenko, *Production of Electron-Positron Pairs by High Energy Photons on Entry Near Crystallographic Planes* (in Russian), Preprint 87–56, Institute of Nuclear Physics, Siberian Division, USSR Academy of Sciences, Novosibirsk, 1987; Nucl. Instrum. Methods **B35**, 21 (1988).

[38] V. V. Tikhomirov, Vestnik Byelorussian State University, Series 1, No. 2, 6, (1983).

[39] J. C. Kimball and N. Cue, Phys. Rev. Lett. **52**, 1747 (1984).

[40] V. N. Baier, V. M. Katkov, and V. M. Strakhovenko, Nucl. Instrum. Methods **B4**, 346 (1984).

[41] V. N. Baĭer, V. M. Katkov, and V. M. Strakhovenko, Zh. Eksp. Teor. Fiz. **63**, 2121 (1972) [Sov. Phys. JETP **36**, 1120 (1973)].

[42] H. Bilokon, G. Bologna, F. Celani, *et al.*, Nucl. Instrum. Methods **204**, 299 (1983).

[43] A. I. Akhiezer and N. F. Shul'ga, Zh. Eksp. Teor. Fiz. **85**, 94 (1983) [Sov. Phys. JETP **58**, 55 (1983)].

[44] H. Bhabha and W. Heitler, Proc. Roy. Soc. **159**, 432 (1937).

[45] J. F. Carlson and J. R. Oppenheimer, Phys. Rev. **51**, 220 (1937).

[46] L. Landau and Yu. Rumer, Proc. Roy. Soc. **166**, 213 (1938).

[47] B. Rossi, *High Energy Particles*, Prentice-hall, 1952. [Russ. Transl. Gostekhteorizdat, M., 1955]

[48] V. N. Baĭer, V. M. Katkov, and V. M. Strakhovenko, Nucl. Instrum. Methods **A250**, 514 (1986).

[49] V. N. Baĭer, V. M. Katkov, and V. M. Strakhovenko, Yad. Fiz. **36**, 163 (1982) [Sov. J. Nucl. Phys. **36**, 95(1982)].

[50] V. N. Baĭer, V. M. Katkov, and V. M. Strakhovenko, Zh. Eksp. Teor. Fiz. **94**, 125 (1988) [Sov. Phys. JETP **67**, 70 (1988)].

[51] V. N. Baĭer, V. M. Katkov, and V. M. Strakhovenko, Phys. Status Solidi Ser. B **149**, 403 (1988).

991   Sov. Phys. Usp. **32** (11), November 1989

Baĭer *et al.*   991

[52]V. G. Baryshevskiĭ and V. V. Tikhomirov, Zh. Eksp. Teor. Fiz. **90**, 1908 (1986) [Sov. Phys. JETP **63**, 1116 (1986)].

[53]V. V. Tichomirov, Phys. Lett. **125A**, 411 (1987).

[54]X. Artru, *ibid.* **128A**, 302 (1988).

[55]A. Belkacem, G. Bologna, M. Chevallier, *et al.*, *Proton Multiplicity in the Hard Radiation of 150 GeV Electrons in an Aligned Germanium Crystal*, Preprint CERN-EP/84–44, Geneva, 1988.

[56]V. I. Ritus, Nucl. Phys. **B44**, 236 (1972).

[57]V. N. Baĭer, V. M. Katkov, and V. M. Strakhovenko, Yad. Fiz. **14**, 1020 (1971) [Sov. J. Nucl. Phys. **14**, 572(1972)].

[58]V. N. Baĭer, A. I. Mil'shteĭn, and R. Zh. Shaĭsultanov, Zh. Eksp. Teor. Fiz. **90**, 1141 (1986) [Sov. Phys. JETP **63**, 665 (1986)].

[59]V. N. Baĭer, A. I. Milstein, and R. Shaisultanov, Phys. Lett. **120A**, 255 (1987).

[60]V. N. Baĭer and V. M. Katkov, Dokl. Akad. Nauk SSSR **171**, 313 (1966) [Sov. Phys. Dokl. **11**, 947 (1967)].

[61]V. V. Lasukov and S. A. Vorobiev, Phys. Lett. **106A**, 179 (1984).

[62]J. C. Kimball and N. Cue, Phys. Rev. Lett. **57**, 1935 (1986).

[63]V. N. Baĭer, V. M. Katkov, and V. M. Strakhovenko, in *Proc. of the Eighth International Conf. on High Energy Particle Accelerators*, Vol. 2, Novosibirsk, 1986.

[64]B. McBreen, Astron. Express. **1**, 105 (1984).

[65]L. I. Ognev, Usp. Fiz. Nauk **154**, 691 (1988) [Sov. Phys. Usp. **31**, 372 (1988)].

Translated by Clark S. Robinson

992   Sov. Phys. Usp. **32** (11), November 1989

Baĭer *et al.*   992